JCTC Journal of Chemical Theory and Computation

An Atomic-Orbital-Based Lagrangian Approach for Calculating Geometric Gradients of Linear Response Properties

Sonia Coriani*

Dipartimento di Scienze Chimiche, Università degli Studi di Trieste, via L. Giorgieri 1, I-34127 Trieste, Italy and Centre for Theoretical and Computational Chemistry, University of Oslo, P.O. Box 1033, N-0315, Blindern, Norway

Thomas Kjærgaard and Poul Jørgensen

Lundbeck Center for Theoretical Chemistry, University of Aarhus, DK-8000 Århus C, Denmark

Kenneth Ruud

Centre for Theoretical and Computational Chemistry (CTCC), Department of Chemistry, University of Tromsø, N-9037 Tromsø, Norway

Joonsuk Huh and Robert Berger

Frankfurt Institute for Advanced Studies (FIAS), Johann Wolfgang Goethe-University, D-60438 Frankfurt am Main, Germany

Received September 25, 2009

Abstract: We present a Lagrangian approach for the calculation of molecular (quadratic) response properties that can be expressed as geometric gradients of a generic linear response function, its poles, and its residues. The approach is implemented within an atomic-orbital-based formalism suitable for linear scaling at the level of self-consistent time-dependent Hartree−Fock and density functional theory. Among the properties that can be obtained using this formalism are the gradient of the frequency-dependent polarizability (e.g., Raman intensities) and that of the one-photon transition dipole moment (entering the Herzberg−Teller factors), in addition to the excited-state molecular forces required for excited-state geometry optimizations. Geometric derivatives of ground-state first-order properties (e.g., IR intensities) and excited-state first-order property expressions are also reported as byproducts of our implementation. The one-photon transition moment gradient is the first analytic implementation of the one-photon transition moment derivative at the DFT level of theory. Besides offering a simple solution to overcome phase (hence, sign) uncertainties connected to the determination of the Herzberg−Teller corrections by numerical derivatives techniques based on independent calculations, our approach also opens the possibility to determine, for example by a mixed analytic−numerical approach, the one-photon transition dipole Hessian, and thus to investigate vibronic effects beyond the linear Herzberg−Teller approximation. As an illustrative application, we report a DFT study of the vibronic fine structure of the one-photon $\tilde{X}(^1A_{1g}) - \tilde{A}(^1B_{2u})$ transition in the absorption spectrum of benzene, which is Franck−Condon-forbidden in the electric dipole approximation and hence determined by the Herzberg−Teller integrals and electronic transition dipole-moment derivatives.

1. Introduction

Derivatives (of electronic properties) with respect to displacements of the nuclei, for brevity denoted as geometric (property) derivatives herein, are one of the key ingredients in describing the effect of molecular vibrations on properties computed within the Born−Oppenheimer approximation, as well as selection rules for a variety of spectroscopic effects, such as Raman or infrared spectroscopy.[1−10] The geometric

* Corresponding author e-mail: coriani@units.it.

10.1021/ct900506c
Published on Web 03/02/2010

derivatives of the dynamic electric dipole polarizability determine, for instance, the intensity of the Raman spectrum[3,9] and play a fundamental role in the theoretical description of other Raman processes, like coherent anti-Stokes Raman Spectroscopy (CARS)[11] and vibrational Raman optical activity.[8,10,12] Similarly, the first geometric derivative of the transition dipole strength yields information on how the motion of the nuclei will affect the UV spectrum (or one-photon absorption, OPA) of a molecule through the so-called Herzberg−Teller (HT) contribution (vibronic coupling between different electronic states).[13−15] Finally, the first geometric derivative of the excited-state energy is the excited-state gradient, which can be used to determine and characterize the equilibrium geometry of a system in an excited electronic state.

Geometric derivatives can be obtained either numerically or analytically. Analytical approaches are more time-consuming to implement in computer codes than numerical methods, but they have the clear advantage of being numerically stable and yielding more accurate results than numerical differentiation, as well as being generally available, once implemented, for any type of system (see, e.g., the discussion in ref 16). Analytic and numerical derivative schemes can also be combined: for instance, the excited-state Hessian can be obtained from the numerical derivative of the analytic excited-state gradient, with higher numerical accuracy than would be obtained in a fully numerical second-order derivative procedure applied to the excited-state energy.

An efficient way to obtain derivatives of a property (usually the energy) is by the Lagrange multipliers technique of multivariable calculus, typically used in constrained optimization problems. The Lagrangian technique has been used in various contexts within the quantum chemistry community, and in electronic structure theory in particular.[9,17−23] A well-known example is the energy/wave-function optimization for both variational and nonvariational wave function approximations, see for instance refs 24 and 25. When implementing analytic geometry derivatives, the Lagrangian technique is used in a nontraditional way, in which the Lagrangian multipliers are treated as wave-function parameters on equal footing with the conventional wave-function parameters. The variational nature of the Lagrangian is then used to reduce the number of response equations that need to be solved. The use of the Lagrangian approach for calculating geometric derivatives was introduced by Helgaker and Jørgensen at the end of the 1980s,[16,18,20] and it has been used, for instance, to obtain the geometric derivatives of ab initio electronic energy surfaces, as well as magnetic derivatives of the energy using perturbation-dependent basis sets.[9,23,26−28] With the introduction of the quasi-energy approach to frequency-dependent response properties,[21,22] the Lagrangian method has been shown to afford efficient computational expressions for the implementation of both dynamic response functions and multiphoton transition moments at various levels of theory, in particular, the coupled-cluster[22,29,30] and, recently, time-dependent density functional[31,32] theories.

In this paper, we use a Lagrangian technique to determine the working equations for third-order molecular properties that are related to the geometric derivatives of second-order response properties—that is, frequency-dependent linear response functions, their poles, and their residues. In the specific case of the electric dipole polarizability and that of the electric-dipole transition strength, these derivatives will correspond to the electric dipole polarizability gradient, which determines the intensity of the Raman spectrum, and to the Herzberg−Teller contribution to the OPA spectrum, respectively. Moreover, as the pole of the linear response function occurs at an electronic excitation from the ground state to an excited state, its geometric first derivative automatically yields the excited-state gradient, and this in turns opens the possibility of obtaining the optimized equilibrium structure of an excited state directly from a ground-state wave function/density.

Since the starting expressions for the second-order quantities to be differentiated are taken according to the atomic orbital formulation of response theory presented in refs 33 and 34—which is based on an exponential parametrization of the atomic-orbital density matrix[25,35]—the resulting properties can be calculated at linear computational cost for sufficiently sparse matrices and can be easily parallelized, since all references to individual two-electron (derivative) integral distributions are avoided and only elementary matrix operations have to be done. The atomic orbital basis we adopt represents a convenient framework for deriving properties whose dependence on the perturbation is already contained in the orbitals. As byproducts of our derivation, we also give the expressions for both the ground- and excited-state first-order properties (e.g., the dipole moments) and the geometric gradient of the ground-state first-order properties (required, for instance, to obtain IR intensities).

Even though we here only consider geometric derivatives, the approach is quite general and has been applied, with a few modifications, to derive and implement working expressions for the magnetic derivatives of second-order properties, using London atomic orbitals to ensure gauge-origin independence.[28] Starting, for instance, from the (imaginary) electric-dipole polarizability and transition strengths, these yield the hyperpolarizability that enters the Verdet constant, and the transition strength that gives the Faraday B term of magneto-optical activity (i.e., the Faraday effect in the transparent and absorptive regions of the sample).[28,36,37] Geometric and magnetic perturbations are treated on an equal footing when using so-called perturbation-dependent basis sets since the atomic orbitals in both of these cases depend explicitly on the differentiating variable. Note, moreover, that the expressions we obtain contain, as a subset, the standard expression for the quadratic response function $\langle\langle A; B, C\rangle\rangle_{\omega,0}$ and its residues when the geometric perturbation is replaced by a generic one-electron (static) operator C.

The procedure we adopt is equivalent to the one used by Furche and co-workers[9,23] to obtain the excited-state gradient and vibrational Raman intensities in time-dependent density functional theory, differing only in that the derivation of Furche and co-workers is expressed in a conventional molecular-orbital basis. Thorvaldsen et al.[32] have also very recently presented a general method for the calculation of molecular properties to arbitrary order, in which the quasienergy and Lagrangian formalisms are combined to derive response functions by differentiation of the quasienergy

derivative Lagrangian using the elements of the density matrix in the atomic orbital representation as variational parameters. The method has been applied to compute, at the Hartree−Fock level, the CARS spectra[11] of a series of polycyclic aromatic hydrocarbons and the vibrational (hyper)-polarizabilities (which require the geometric gradients of the electric dipole moment, electric polarizability, and electric first hyperpolarizability) of water, of three all-trans polyenes, and of three 4-dimethylaminophenylpolyene aldehydes.[38] Excited-state and (hyper)polarizability gradient implementations have thus been reported previously, while this work presents the first implementation of the analytic computation of the transition moment derivatives. We also note that the analytic evaluation of transition moment derivatives offers a simple solution to overcome phase (hence, sign) uncertainties connected to the their determination by numerical derivatives techniques based on totally independent calculations. In principle, it can also be combined with a numerical differentiation scheme, as commonly done to determine the excited-state Hessian, to yield the transition-moment second-order derivates, allowing the investigation of vibronic effects beyond the linear Herzberg−Teller approximation (note however that, in such mixed numerical−analytical schemes for transition moments, the phase uncertainties may re-emerge).

This paper is organized as follows. In the Theory section, we first define the key quantities which represent the formal background for our derivation. We then outline the Lagrange method both in general terms and in a more specific way for the properties of interest. The implemented expressions for the second-order property derivatives (third-order properties) will be given at the end of the section.

As an illustrative application, we report in the Illustrative Results section an exhaustive DFT study of the vibronic fine structure of the one-photon $\tilde{X}(^1A_{1g}) - \tilde{A}(^1B_{2u})$ transition in the absorption spectrum of benzene. This transition is Franck−Condon-forbidden in the electric dipole approximation and hence dominated by the (first-order) Herzberg−Teller integrals and electronic transition dipole-moment derivatives.[13,39]

2. Theory

2.1. Ansatz: Exponential Parametrization of the Density. We start by assuming that the wave function (or density) of the ground state is optimized for a point on the potential surface ($\mathbf{R}_0$) such that the variational condition at that point is fulfilled:[40]

$$\mathbf{E}^{[1]} = \mathbf{FDS} - \mathbf{SDF} = \mathbf{0} \tag{1}$$

where $\mathbf{E}^{[1]}$ is the matrix representation of the electronic gradient in the nonorthogonal atomic orbital (AO) basis, $\mathbf{S}$ is the AO overlap matrix, $\mathbf{D}$ is the AO density, and $\mathbf{F}$ is the Fock/Kohn−Sham matrix:

$$\mathbf{F} = \mathbf{h} + \mathbf{G}^{\mathrm{HF}}(\mathbf{D}) \tag{2}$$

In the equation above, $\mathbf{h}$ is the AO integral matrix for the one-electron part (kinetic plus nuclear attraction) of the Hamilton operator and $\mathbf{G}(\mathbf{D})$ denotes the Coulomb and exact-exchange contributions:

$$G^{\mathrm{HF}}_{\mu\nu}(\mathbf{D}) = \sum_{\rho\sigma} D_{\sigma\rho}[g_{\mu\nu\rho\sigma} - w_x g_{\mu\sigma\rho\nu}] \tag{3}$$

The scaling factor w_x is equal to 1 for Hartree−Fock. In the case of Kohn−Sham theory, the scaling factor w_x is zero unless a hybrid functional is used, and an additional contribution from the exchange-correlation potential must be included in the Kohn−Sham matrix,[41]

$$\mathbf{F} = \mathbf{h} + \mathbf{G}^{\mathrm{HF}}(\mathbf{D}) + \mathbf{F}^{\mathrm{xc}} \tag{4}$$

The last term in eq 4 is the derivative of the exchange-correlation functional $E_{\mathrm{xc}}[\rho]$:

$$F^{\mathrm{xc}}_{\mu\nu} = \frac{\partial E_{\mathrm{xc}}[\rho]}{\partial D_{\nu\mu}} \tag{5}$$

Expressing the density ρ in the AO basis as

$$\rho(\mathbf{r}) = \sum_{\mu\nu} \chi^*_\mu(\mathbf{r})\, \chi_\nu(\mathbf{r})\, D_{\nu\mu} = \sum_{\mu\nu} \Omega_{\mu\nu}(\mathbf{r})\, D_{\nu\mu} \tag{6}$$

where $\Omega_{\mu\nu}(\mathbf{r}) = \chi^*_\mu(\mathbf{r})\, \chi_\nu(\mathbf{r})$ is the overlap distribution, and introducing the exchange-correlation potential

$$v_{\mathrm{xc}}(\mathbf{r}) = \frac{\delta E_{\mathrm{xc}}[\rho]}{\delta \rho(\mathbf{r})} \tag{7}$$

we see that

$$F^{\mathrm{xc}}_{\mu\nu} = \int \frac{\delta E_{\mathrm{xc}}[\rho]}{\delta \rho(\mathbf{r})} \frac{\partial \rho(\mathbf{r})}{\partial D_{\nu\mu}}\, \mathrm{d}\mathbf{r} = \int v_{\mathrm{xc}}(\mathbf{r})\, \Omega_{\mu\nu}(\mathbf{r})\, \mathrm{d}\mathbf{r} \tag{8}$$

The ground-state energy at $\mathbf{R}_0$ is obtained as

$$E_0 = \mathrm{Tr}\, \mathbf{hD} + \frac{1}{2}\mathrm{Tr}\, \mathbf{DG}^{\mathrm{HF}}(\mathbf{D}) + E_{\mathrm{xc}}[\rho] + h_{\mathrm{nuc}} \tag{9}$$

where h_{nuc} is the nuclear repulsion term.

The variational condition in the form given in eq 1—as well as the response expressions in the next sections—was derived on the basis of an exponential parametrization of the AO density matrix:[25,33,35,40]

$$\mathbf{D}(\mathbf{X}) = \exp(-\mathbf{XS})\mathbf{D}\exp(\mathbf{SX}) = \mathbf{D} + [\mathbf{D}, \mathbf{X}]_{\mathrm{S}} + \frac{1}{2}[[\mathbf{D}, \mathbf{X}]_{\mathrm{S}}, \mathbf{X}]_{\mathrm{S}} + \ldots \tag{10}$$

where $\mathbf{X}$ is an anti-Hermitian matrix that contains the variational parameters, with the redundant parameters projected out:

$$\mathbf{X} = \mathscr{P}(\mathbf{X}) \equiv \mathbf{P}_{\mathrm{o}}\mathbf{X}\mathbf{P}_{\mathrm{v}}^{\mathrm{T}} + \mathbf{P}_{\mathrm{v}}\mathbf{X}\mathbf{P}_{\mathrm{o}}^{\mathrm{T}} \tag{11}$$

$\mathbf{P}_{\mathrm{o}}$ and $\mathbf{P}_{\mathrm{v}}$ are projectors onto the occupied and virtual orbital spaces, respectively:

$$\mathbf{P}_{\mathrm{o}} = \mathbf{DS} \tag{12}$$

$$\mathbf{P}_{\mathrm{v}} = \mathbf{I} - \mathbf{DS} \tag{13}$$

fulfilling the idempotency ($\mathbf{P}_{\mathrm{o}}^2 = \mathbf{P}_{\mathrm{o}}$ and $\mathbf{P}_{\mathrm{v}}^2 = \mathbf{P}_{\mathrm{v}}$) and orthogonality relations ($\mathbf{P}_{\mathrm{o}}\mathbf{P}_{\mathrm{v}} = \mathbf{P}_{\mathrm{v}}\mathbf{P}_{\mathrm{o}} = \mathbf{0}$ and $\mathbf{P}_{\mathrm{o}}^{\mathrm{T}}\mathbf{S}\mathbf{P}_{\mathrm{v}} = \mathbf{P}_{\mathrm{v}}^{\mathrm{T}}\mathbf{S}\mathbf{P}_{\mathrm{o}} = \mathbf{0}$). The so-called S commutator appearing in eq 10 is defined as

$$[\mathbf{D}, \mathbf{X}]_S = \mathbf{DSX} - \mathbf{XSD} \tag{14}$$

More generally, we introduce the M commutator as

$$[\mathbf{L}, \mathbf{N}]_M = \mathbf{LMN} - \mathbf{NML} \tag{15}$$

2.2. A Few Words on Notation. Before proceeding, it is convenient to introduce here a more compact notation, which is repeatedly used throughout the paper. According to it, we write an element of the gradient matrix in eq 1 as[33]

$$E_m^{[1]} = \mathrm{Tr}\, \mathbf{F}[\mathbf{D}, \mathbf{O}_m^\dagger]_S = \mathrm{Tr}\, \mathbf{O}_m^\dagger(\mathbf{FDS} - \mathbf{SDF}) \equiv \mathrm{Tr}\, \mathbf{O}_m^\dagger \mathbf{E}^{[1]} \tag{16}$$

As a rule of thumb, we can go from the (element-wise) notation to the true matrix representation in the AO basis using

$$M_j = \mathrm{Tr}\, \mathbf{O}_j^\dagger \mathbf{M} \tag{17}$$

where the index j indicates a $M_{\mu\nu}$ element of the matrix $\mathbf{M}$ in the AO basis. The operator $\mathbf{O}_j^\dagger$ and its adjoint $\mathbf{O}_j$ are defined in ref 33. We also introduce here the expansions

$$\mathbf{b}^\omega = \sum_m b_m^\omega \mathbf{O}_m; \qquad \mathbf{b}^{\omega\dagger} = \sum_m b_m^{\omega *} \mathbf{O}_m^\dagger \tag{18}$$

2.3. Ansatz: AO-Based Linear Response Theory. We consider now the expansion of the time-dependent expectation value of a time-independent operator A with respect to a (periodic) perturbation $V^t = \int_{-\infty}^{+\infty} V^\omega \exp(-i\omega t)\, \mathrm{d}\omega$:

$$\langle A(t) \rangle = A_0 + \int \langle\langle A; V^\omega \rangle\rangle_\omega \exp(-i\omega t)\, \mathrm{d}\omega + \ldots \tag{19}$$

where $\langle\langle A; V^\omega \rangle\rangle_\omega$ is the linear response function. Assuming implicit summation over repeated indices, and introducing the symbol B in place of V^ω, the linear response function (LRF) is given by[33]

$$\langle\langle A;B \rangle\rangle_\omega = -A_m^{[1]} b_m^\omega = -\boldsymbol{A}^{[1]\dagger} \boldsymbol{b}^\omega \equiv -\mathrm{Tr}(\mathbf{A}^{[1]\dagger} \mathbf{b}^\omega) = + \mathrm{Tr}\mathbf{A}[\mathbf{b}^\omega, \mathbf{D}]_S \tag{20}$$

where the elements b_m^ω of the response "vector" $\boldsymbol{b}^\omega$ (matrix $\mathbf{b}^\omega$) are obtained from the solution of the linear response equation

$$(E_{mn}^{[2]} - \omega S_{mn}^{[2]}) b_n^\omega = B_m^{[1]} \tag{21}$$

or, in supermatrix notation,[28]

$$(\boldsymbol{E}^{[2]} - \omega \boldsymbol{S}^{[2]}) \boldsymbol{b}^\omega = \boldsymbol{B}^{[1]} \tag{22}$$

and where

$$A_m^{[1]} = -\mathrm{Tr}\, \mathbf{A}[\mathbf{O}_m, \mathbf{D}]_S \tag{23}$$

$$\mathbf{A}^{[1]} = \mathbf{SDA}^\dagger - \mathbf{A}^\dagger \mathbf{DS} \tag{24}$$

is the *property gradient* relative to the A operator (whose expectation value is perturbed). The right-hand side of the linear response equation is the *property gradient* relative to the external perturbation described by the V^ω ($\equiv B$) operator,

$$B_m^{[1]} = \mathrm{Tr}\, \mathbf{B}[\mathbf{D}, \mathbf{O}_m^\dagger]_S = \mathrm{Tr}\, \mathbf{O}_m^\dagger(\mathbf{BDS} - \mathbf{SDB}) \tag{25}$$

$$\mathbf{B}^{[1]} = \mathbf{BDS} - \mathbf{SDB} \tag{26}$$

$\boldsymbol{E}^{[2]}$ and $\boldsymbol{S}^{[2]}$ are the generalized electronic Hessian and metric matrices in the AO basis:[33]

$$E_{mn}^{[2]} = \mathrm{Tr}\, \mathbf{F}[[\mathbf{O}_n, \mathbf{D}]_S, \mathbf{O}_m^\dagger]_S + \mathrm{Tr}\, \mathbf{G}([\mathbf{O}_n, \mathbf{D}]_S)[\mathbf{D}, \mathbf{O}_m^\dagger]_S \tag{27}$$

$$S_{mn}^{[2]} = \mathrm{Tr}\, \mathbf{O}_m^\dagger \mathbf{S}[\mathbf{D}, \mathbf{O}_n]_S \mathbf{S} \equiv -\mathrm{Tr}\, \mathbf{O}_m^\dagger \mathbf{S}[\mathbf{O}_n, \mathbf{D}]_S \mathbf{S} \tag{28}$$

where we define

$$\mathbf{G}(\mathbf{M}) = \mathbf{G}^{\mathrm{HF}}(\mathbf{M}) + \mathbf{G}^{\mathrm{xc}}(\mathbf{M}) \tag{29}$$

and introduce the matrix[41]

$$G_{\mu\nu}^{\mathrm{xc}}(\mathbf{M}) = \sum_{\rho\sigma} M_{\sigma\rho} \int \frac{\delta^2 E^{\mathrm{xc}}}{\delta\rho(\mathbf{s})\, \delta\rho(\mathbf{r})} \Omega_{\mu\nu}(\mathbf{r})\, \Omega_{\rho\sigma}(\mathbf{s})\, \mathrm{d}\mathbf{r}\, \mathrm{d}\mathbf{s} \tag{30}$$

Note that the elements of the (super)matrix $\boldsymbol{E}^{[2]}$ are here defined so that $\boldsymbol{E}^{[2]}$ is positive definite.

The linear response function has poles whenever the frequency ω is equal to an excitation energy ω_f. The excitation energies ω_f and excitation vectors $\boldsymbol{b}^f$ (matrices $\mathbf{b}^f$) are obtained from the solution of the generalized eigenvalue equation

$$(\boldsymbol{E}^{[2]} - \omega_f \boldsymbol{S}^{[2]}) \boldsymbol{b}^f = \mathbf{0} \tag{31}$$

The corresponding residue of the linear response function can be shown to be[34]

$$\lim_{\omega \to \omega_f} (\omega - \omega_f) \langle\langle A;B \rangle\rangle_\omega = (\boldsymbol{A}^{[1]\dagger} \boldsymbol{b}^f)(\boldsymbol{b}^{f\dagger} \boldsymbol{B}^{[1]}) = \mathrm{Tr}(\mathbf{A}^{[1]\dagger} \mathbf{b}^f)\, \mathrm{Tr}(\mathbf{b}^{f\dagger} \mathbf{B}^{[1]}) \tag{32}$$

Note that the excited-state vector is normalized on the generalized metric matrix $\boldsymbol{S}^{[2]}$, that is

$$\boldsymbol{b}^{f\dagger} \boldsymbol{S}^{[2]} \boldsymbol{b}^f = 1 \tag{33}$$

and that $\boldsymbol{S}^{[2]}$ is *not* positive definite.

2.4. Construction of the Lagrangian and Variational Condition. One obvious way to obtain our third-order properties would be a straightforward differentiation of the second-order property expressions previously given. However, such an approach would automatically imply that derivatives of (either or both) the linear response vectors ($\boldsymbol{b}^\omega$) and the eigenvectors ($\boldsymbol{b}^f$) would be required. Hence, additional equations depending (often in a rather complicated fashion) on the number of external perturbations (up to $3N$ for each component) should be solved. Such an approach has an evident drawback when dealing with properties of large systems, as the number of equations to be solved would quickly become too large to be handled.

Alternatively, computationally efficient expressions for the third-order molecular properties can be obtained using a Lagrangian technique.[16,17,19] For each second-order property (component) $\mathcal{C}$ we want to differentiate—either a linear response function, a transition moment, or an excitation

energy—we construct a Lagrangian function (component) $\mathscr{L}$, adding to the second-order property in question the appropriate constraint equations that must be satisfied, each multiplied by a set of Lagrange multipliers:

$$\mathscr{L}(\mathbf{R},\boldsymbol{\lambda},\bar{\boldsymbol{\lambda}},\mathbf{X},\bar{\mathbf{X}}) = \mathscr{O}(\mathbf{R},\boldsymbol{\lambda},\mathbf{X}) + \sum_m \bar{\lambda}_m \mathscr{P}_m(\mathbf{R},\boldsymbol{\lambda},\mathbf{X}) + \sum_n \bar{X}_m \mathscr{O}_n(\mathbf{R},\mathbf{X}) \quad (34)$$

where $\boldsymbol{\lambda} = \boldsymbol{\lambda}(\mathbf{R})$ collectively represent the "property parameters" (for instance, the response and excitation vectors), $\mathbf{X} = \mathbf{X}(\mathbf{R})$ are the "orbital parameters" [see eq 11], $\bar{\boldsymbol{\lambda}}(\mathbf{R})$ are the Lagrange multipliers connected to the property parameters (or property constraints $\mathscr{P} = 0$), and $\bar{\mathbf{X}}(\mathbf{R})$ are the Lagrange multipliers related to the orbital parameters (or orbital constraints $\mathscr{O} = 0$). The variable $\mathbf{R}$ collectively indicates the spatial coordinates of the nuclei. Note the dependence of the property constraint equations on both the spatial coordinates of the nuclei $\mathbf{R}$, the property parameters $\boldsymbol{\lambda}$, *and* the orbital parameters $\mathbf{X}$.

Next, we make the Lagrangian fully variational, imposing its stationarity with respect to any variation in both property/orbital parameters and Lagrange multipliers ($\forall i$, $\mathbf{R}$)

$$\frac{\partial \mathscr{L}(\mathbf{R},\boldsymbol{\lambda},\bar{\boldsymbol{\lambda}},\mathbf{X},\bar{\mathbf{X}})}{\partial \bar{\lambda}_i} = 0 \leftrightarrow \mathscr{P}_i(\mathbf{R},\boldsymbol{\lambda},\mathbf{X}) = 0 \quad (35a)$$

$$\frac{\partial \mathscr{L}(\mathbf{R},\boldsymbol{\lambda},\bar{\boldsymbol{\lambda}},\mathbf{X},\bar{\mathbf{X}})}{\partial \lambda_i} = 0 \leftrightarrow \frac{\partial \mathscr{O}(\mathbf{R},\boldsymbol{\lambda},\mathbf{X})}{\partial \lambda_i} + \sum_j \bar{\lambda}_j \frac{\partial \mathscr{P}_j(\mathbf{R},\boldsymbol{\lambda},\mathbf{X})}{\partial \lambda_i} = 0 \quad (35b)$$

$$\frac{\partial \mathscr{L}(\mathbf{R},\boldsymbol{\lambda},\bar{\boldsymbol{\lambda}},\mathbf{X},\bar{\mathbf{X}})}{\partial \bar{X}_i} = 0 \leftrightarrow \mathscr{O}_i(\mathbf{R},\mathbf{X}) = 0 \quad (35c)$$

$$\frac{\partial \mathscr{L}(\mathbf{R},\boldsymbol{\lambda},\bar{\boldsymbol{\lambda}},\mathbf{X},\bar{\mathbf{X}})}{\partial X_i} = 0 \leftrightarrow \frac{\partial \mathscr{O}(\mathbf{R},\boldsymbol{\lambda},\mathbf{X})}{\partial X_i} + \sum_j \bar{\lambda}_j \frac{\partial \mathscr{P}_j(\mathbf{R},\boldsymbol{\lambda},\mathbf{X})}{\partial X_i} + \sum_j \bar{X}_j \frac{\partial \mathscr{O}_j(\mathbf{R},\mathbf{X})}{\partial X_i} = 0 \quad (35d)$$

Equations 35a and 35c simply correspond to the constraint equations that determine the property parameters ($\boldsymbol{\lambda}$) and orbital parameters ($\mathbf{X}$), respectively. Equation 35b can be used to determine the property Lagrange multipliers ($\bar{\boldsymbol{\lambda}}$), whereas eq 35d affords the orbital Lagrange multipliers ($\bar{\mathbf{X}}$).

Finally, we obtain the properties of interest from the derivative of the Lagrangian with respect to the displacements of the nuclei. For the values of the parameters that satisfy eqs 35a to 35d, it yields

$$\left.\frac{\mathrm{d}\mathscr{L}(\mathbf{R},\boldsymbol{\lambda},\bar{\boldsymbol{\lambda}},\mathbf{X},\bar{\mathbf{X}})}{\mathrm{d}R_\beta}\right|_{\mathbf{R}_0} = \left.\frac{\partial \mathscr{L}(\mathbf{R},\boldsymbol{\lambda},\bar{\boldsymbol{\lambda}},\mathbf{X},\bar{\mathbf{X}})}{\partial R_\beta}\right|_{\mathbf{R}_0} = \left.\frac{\partial \mathscr{O}(\mathbf{R},\boldsymbol{\lambda},\mathbf{X})}{\partial R_\beta}\right|_{\mathbf{R}_0} + \left.\sum_i \bar{\lambda}_i \frac{\partial \mathscr{P}_i(\mathbf{R},\boldsymbol{\lambda},\mathbf{X})}{\partial R_\beta}\right|_{\mathbf{R}_0} + \left.\sum_i \bar{X}_i \frac{\partial \mathscr{O}_i(\mathbf{R},\mathbf{X})}{\partial R_\beta}\right|_{\mathbf{R}_0} \equiv \left.\frac{\mathrm{d}\mathscr{O}(\mathbf{R},\boldsymbol{\lambda},\mathbf{X})}{\mathrm{d}R_\beta}\right|_{\mathbf{R}_0} \quad (36)$$

(with $R_\beta \in \mathbf{R}$ indicating one specific spatial coordinate of the nuclei). Third-order molecular properties are thus conveniently formulated as derivatives of the variational linear-response property Lagrangian. Using the Lagrangian technique, we thus replace the calculation of the parameters' response with respect to each perturbation R_β with the calculation of the Lagrangian multipliers, that is, one additional set of equations (eq 35b) for each λ_i independent of the number of perturbations (and similarly for the orbital parameters X_i).

In practice, the solution of eqs 35a−35d, and consequent calculation of the properties according to eq 36 and its higher-order analogs, is carried out within a variational perturbation theory approach[16] by expanding the parameters in order of the (external) perturbation. When the expansions are inserted in the expressions for the property or property Lagrangian, variational conditions for each order of the perturbation are obtained in place of one condition for each value of the field.[16] In this way, molecular properties are obtained in accordance with Wigner's $2n + 1$ rule for the parameters (the parameter response to order n determines the property derivatives to order $2n + 1$), as well as the stronger $2n + 2$ rule for the multipliers.[16] Due to the $(2n + 1)$ rule, and since the properties considered here are first-order properties with respect to the displacement of the nuclei, we only need to solve the above equations through zeroth order in the displacements.

We now go into detail and report explicit expressions for the various quantities entering eq 36 for the properties of interest to us.

2.4.1. The Linear Response Function Lagrangian. For the linear response function, the property Lagrangian is

$$\begin{aligned}\mathscr{L}^{\alpha} &= -A_m^{[1]} b_m^{\omega} + \bar{\lambda}_m^{*}(E_{mj}^{[2]} b_j^{\omega} - \omega S_{mj}^{[2]} b_j^{\omega} - B_m^{[1]}) - \bar{X}_m^{*} E_m^{[1]} \\ &\equiv -\boldsymbol{A}^{[1]\dagger}\boldsymbol{b}^{\omega} + \bar{\boldsymbol{\lambda}}^{\dagger}(\boldsymbol{E}^{[2]}\boldsymbol{b}^{\omega} - \omega \boldsymbol{S}^{[2]}\boldsymbol{b}^{\omega} - \boldsymbol{B}^{[1]}) - \bar{\boldsymbol{X}}^{\dagger}\boldsymbol{E}^{[1]}\end{aligned} \quad (37)$$

where the second equality is again given in a supermatrix notation. It is apparent that the parameter constraint equation corresponds to the linear response equation determining $\boldsymbol{b}^{\omega}$. The orbital constraint equation in eq 34 corresponds to the optimization condition that determines the orbital parameters $\mathbf{X}$, already given in eqs 16 and 1.

2.4.2. The Residue Lagrangian. For the residue (i.e., the one-photon transition moment),

$$\begin{aligned}\mathscr{L}^{S} = A_m^{[1]} b_m^{f} - \bar{\lambda}_m^{*}(E_{mj}^{[2]} b_j^{f} - \omega_f S_{mj}^{[2]} b_j^{f}) - \bar{\omega}(b_m^{f*} S_{mj}^{[2]} b_j^{f} - 1) - \bar{X}_m^{*} E_m^{[1]} \equiv \boldsymbol{A}^{[1]\dagger}\boldsymbol{b}^{f} - \bar{\boldsymbol{\lambda}}^{\dagger}(\boldsymbol{E}^{[2]}\boldsymbol{b}^{f} - \omega_f \boldsymbol{S}^{[2]}\boldsymbol{b}^{f}) - \\ \bar{\omega}(\boldsymbol{b}^{f\dagger}\boldsymbol{S}^{[2]}\boldsymbol{b}^{f} - 1) - \bar{\boldsymbol{X}}^{\dagger}\boldsymbol{E}^{[1]}\end{aligned} \quad (38)$$

Note that in this case we have two "parameter" constraint equations, namely, the generalized eigenvalue equation for the excited-state vector $\boldsymbol{b}^{f}$, eq 31, and the orthonormality condition on the same excited-state vector, eq 33. The orbital constraint equation is obviously the same as for the linear response function Lagrangian.

2.4.3. The Excited State Energy Lagrangian. Last, for the excited-state energy, $E_f = E_0 + \omega_f$, we have

$$\mathscr{L}^{E_f} = E_0 + b_m^{f*}E_{mj}^{[2]}b_j^f - \bar{\omega}(b_m^{f*}S_{mj}^{[2]}b_j^f - 1) - \bar{X}_m E_m^{[1]}$$
$$\equiv E_0 + \boldsymbol{b}^{f\dagger}\boldsymbol{E}^{[2]}\boldsymbol{b}^f - \bar{\omega}(\boldsymbol{b}^{f\dagger}\boldsymbol{S}^{[2]}\boldsymbol{b}^f - 1) - \bar{\boldsymbol{X}}^{\dagger}\boldsymbol{E}^{[1]} \quad (39)$$

where the excitation frequency ω_f was rewritten as

$$\omega_f = b_m^{f*}E_{mj}^{[2]}b_j^f \equiv \boldsymbol{b}^{f\dagger}\boldsymbol{E}^{[2]}\boldsymbol{b}^f \quad (40)$$

and the orthonormalization condition on the excited-state vectors in eq 33 was used as a unique constraint equation.

2.4.4. The Variational Conditions for the LRF Lagrangian. It is instructive to analyze the specific outcome of the application of the variational conditions with respect to the parameters and multipliers on the three Lagrangian functions above. Thus, for the linear response function

$$\frac{\partial\mathscr{L}}{\partial\bar{X}_j^*} = 0 \leftrightarrow E_j^{[1]} = 0 \quad (41a)$$

$$\frac{\partial\mathscr{L}}{\partial\bar{\lambda}_j^*} = 0 \leftrightarrow E_{jl}^{[2]}b_l^{\omega} - \omega S_{jl}^{[2]}b_l^{\omega} = B_j^{[1]} \quad (41b)$$

$$\frac{\partial\mathscr{L}}{\partial b_j^{\omega}} = 0 \leftrightarrow A_j^{[1]} = \bar{\lambda}_m^*(E_{mj}^{[2]} - \omega S_{mj}^{[2]}) \quad (41c)$$

$$\frac{\partial\mathscr{L}}{\partial X_j} = 0 \leftrightarrow -\frac{\partial A_m^{[1]}}{\partial X_j}b_m^{\omega} + \bar{\lambda}_m^*\frac{\partial E_{ml}^{[2]}}{\partial X_j}b_l^{\omega} - \omega\bar{\lambda}_m^*\frac{\partial S_{ml}^{[2]}}{\partial X_j}b_l^{\omega} - \bar{\lambda}_m^*\frac{\partial B_m^{[1]}}{\partial X_j} = \bar{X}_m^*\frac{\partial E_m^{[1]}}{\partial X_j} \quad (41d)$$

It can be easily recognized that eq 41c corresponds to a *transposed* linear response equation, as used for instance to determine the $\boldsymbol{a}^{\omega}$ (or $N^A(\omega)$) vector of the quadratic response function,[41−43] that is, $\bar{\boldsymbol{\lambda}}^{\dagger} = \boldsymbol{a}^{\omega\dagger}$. Since our response solver[34] performs the linear transformation from the right, the $\boldsymbol{\lambda}^{\dagger}$ multipliers are instead obtained by solving

$$(\boldsymbol{E}^{[2]} - \omega\boldsymbol{S}^{[2]})\bar{\boldsymbol{\lambda}} = \boldsymbol{A}^{[1]} \quad (42)$$

and then *taking the adjoint* of the resulting vector (matrix) $\bar{\boldsymbol{\lambda}}$.

The equation that determines the orbital Lagrangian multipliers, eq 41d, will be discussed in section 2.5 together with the corresponding ones from the transition-moment and excitation-energy Lagrangians.

2.4.5. The Variational Conditions for the Residue Lagrangian. For the transition-moment Lagrangian, we have

$$\frac{\partial\mathscr{L}}{\partial\bar{X}_j^*} = 0 \leftrightarrow E_j^{[1]} = 0 \quad (43a)$$

$$\frac{\partial\mathscr{L}}{\partial\bar{\omega}} = 0 \leftrightarrow b_m^{f*}S_{mj}^{[2]}b_j^f = 1 \quad (43b)$$

$$\frac{\partial\mathscr{L}}{\partial\bar{\lambda}_j^*} = 0 \leftrightarrow E_{ji}^{[2]}b_i^f - \omega_f S_{ji}^{[2]}b_i^f = 0 \quad (43c)$$

$$\frac{\partial\mathscr{L}}{\partial b_j^f} = 0 \leftrightarrow A_j^{[1]} = \bar{\lambda}_m^*(E_{mj}^{[2]} - \omega_f S_{mj}^{[2]}) + 2\bar{\omega}b_m^{f*}S_{mj}^{[2]} \quad (43d)$$

$$\frac{\partial\mathscr{L}}{\partial X_j} = 0 \leftrightarrow \frac{\partial A_m^{[1]}}{\partial X_j}b_m^f - \bar{\lambda}_m^*\frac{\partial E_{ml}^{[2]}}{\partial X_j}b_l^f + \omega_f\bar{\lambda}_m^*\frac{\partial S_{ml}^{[2]}}{\partial X_j}b_l^f - \bar{\omega}b_m^{f*}\frac{\partial S_{ml}^{[2]}}{\partial X_j}b_l^f = \bar{X}_m^*\frac{\partial E_m^{[1]}}{\partial X_j} \quad (43e)$$

Equations 43c and 43e are clearly the eigenvalue equation and orbital parameter equation, respectively.

Equation 43d requires special attention. Similar to what was done for the linear response function, we solve the adjoint equation:

$$(\boldsymbol{E}^{[2]} - \omega_f\boldsymbol{S}^{[2]})\bar{\boldsymbol{\lambda}} + 2\bar{\omega}\boldsymbol{S}^{[2]}\boldsymbol{b}^f = \boldsymbol{A}^{[1]} \quad (44)$$

This is a linear-response equation, though for a frequency ω equal to an excitation frequency ω_f. Since the excitation energy is a pole of the resolvent matrix $(\boldsymbol{E}^{[2]} - \omega_f\boldsymbol{S}^{[2]})$, eq 43d is divergent with the solution vector $\bar{\boldsymbol{\lambda}}$ having an undefined component along the excitation vector $\boldsymbol{b}^f$. By multiplying from the left with $\boldsymbol{b}^{f\dagger}$, we decouple $\bar{\omega}$ from $\bar{\lambda}$ and determine the value of the multiplier $\bar{\omega}$

$$\bar{\omega} = \frac{1}{2}\boldsymbol{b}^{f\dagger}\boldsymbol{A}^{[1]} \quad (45)$$

since $\boldsymbol{b}^{f\dagger}(\boldsymbol{E}^{[2]} - \omega_f\boldsymbol{S}^{[2]}) = \boldsymbol{0}$. Multiplying with the orthogonal complement of $\boldsymbol{b}^{f\dagger}$, which is represented by the (projection) matrix

$$\boldsymbol{P}_f^{\dagger} = \boldsymbol{I} - \boldsymbol{S}^{[2]}\boldsymbol{b}^f\boldsymbol{b}^{f\dagger} \quad (46)$$

gives

$$\boldsymbol{P}_f^{\dagger}[(\boldsymbol{E}^{[2]} - \omega_f\boldsymbol{S}^{[2]})\bar{\boldsymbol{\lambda}}] = \boldsymbol{P}_f^{\dagger}\boldsymbol{A}^{[1]} \quad (47)$$

If we now partition the solution vector $\bar{\boldsymbol{\lambda}}$ as

$$\bar{\boldsymbol{\lambda}} = \boldsymbol{P}_f\bar{\boldsymbol{\lambda}} + \gamma\boldsymbol{b}^f \quad (48)$$

with

$$\boldsymbol{P}_f = \boldsymbol{I} - \boldsymbol{b}^f\boldsymbol{b}^{f\dagger}\boldsymbol{S}^{[2]} \quad (49)$$

and introduce it in the response equation eq 44, we are left with the well-defined, nondivergent response equation

$$\boldsymbol{P}_f^{\dagger}\{(\boldsymbol{E}^{[2]} - \omega_f\boldsymbol{S}^{[2]})\boldsymbol{P}_f(\bar{\boldsymbol{\lambda}})\} = \boldsymbol{P}_f^{\dagger}(\boldsymbol{A}^{[1]}) \quad (50)$$

since the contribution along $\boldsymbol{b}^f$ automatically vanishes because of eq 31.

In practice, eq 50 is solved by means of an iterative procedure based on trial vectors, and we need to ensure that the solution vector is kept orthogonal to the excitation vector at each step in the iterative procedure.

Since our solver[34] exploits a paired structure, where the trial vectors are normalized and orthogonalized against each other in a standard Euclidian way, the basis of trial vectors is chosen as a $2 + 2n$ basis, where the first two vectors are always chosen as the excitation vector $\boldsymbol{b}^f$, and its paired counterpart $\boldsymbol{b}^{-f}$. The remaining $2n$ vectors are generated as in the standard procedure,[34] but with the additional requirement that they are always kept orthogonal, in terms of an $\boldsymbol{S}^{[2]}$ norm, to both $\boldsymbol{b}^f$ and $\boldsymbol{b}^{-f}$

$$\boldsymbol{b}_i = (\boldsymbol{I} - \boldsymbol{b}^f\boldsymbol{b}^{f\dagger}\boldsymbol{S}^{[2]} - \boldsymbol{b}^{-f}\boldsymbol{b}^{-f\dagger}\boldsymbol{S}^{[2]})\boldsymbol{b}_i;\ \forall i = 3,\ ...,\ 2n + 2 \tag{51}$$

We refer to ref 28 for a detailed discussion of the algorithm.

2.4.6. The Variational Conditions for the Excited-State Energy Lagrangian. Finally, for the excited-state energy Lagrangian,

$$\frac{\partial \mathscr{L}}{\partial \bar{X}_j^*} = 0 \leftrightarrow E_j^{[1]} = 0 \tag{52a}$$

$$\frac{\partial \mathscr{L}}{\partial \bar{\omega}} = 0 \leftrightarrow b_j^{f*} S_{ji}^{[2]} b_i^f - 1 = 0 \tag{52b}$$

$$\frac{\partial \mathscr{L}}{\partial b_i^f} = 0 \leftrightarrow 2(E_{ji}^{[2]} b_i^f - \bar{\omega} S_{ji}^{[2]} b_i^f) = 0 \tag{52c}$$

$$\frac{\partial \mathscr{L}}{\partial X_j} = 0 \leftrightarrow \frac{\partial E_0}{\partial X_j} + b_m^f \frac{\partial E_{ml}^{[2]}}{\partial X_j} b_l^f - \bar{\omega} b_m^{f*} \frac{\partial S_{ml}^{[2]}}{\partial X_j} b_l^f = \bar{X}_m^* \frac{\partial E_m^{[1]}}{\partial X_j} \tag{52d}$$

which allows us to identify $\bar{\omega} = \omega_f$.

2.5. The Response Equations for "Orbital" Lagrange Multipliers $\bar{\mathbf{X}}$. For the determination of the orbital Lagrange multipliers in the three cases, we need to solve eqs 41d, 43e, and 52d, respectively. They involve the derivatives with respect to each orbital parameter X_i of the elements of the generalized Hessian ($\boldsymbol{E}^{[2]}$) and metric ($\boldsymbol{S}^{[2]}$) matrices, as well as of the property gradients ($\boldsymbol{A}^{[1]\dagger}$ and/or $\boldsymbol{B}^{[1]}$) and of the electronic gradient ($\boldsymbol{E}^{[1]}$). These can be shown to correspond to

$$\frac{\partial E_m^{[1]}}{\partial X_j} \Rightarrow E_{mj}^{[2]} \tag{53}$$

$$\frac{\partial B_m^{[1]}}{\partial X_j} \Rightarrow B_{mj}^{[2]} = -\mathrm{Tr}\, \mathbf{B}[[\mathbf{O}_j, \mathbf{D}]_\mathrm{S}, \mathbf{O}_m^\dagger]_\mathrm{S} \tag{54}$$

$$\frac{\partial A_m^{[1]}}{\partial X_j} \Rightarrow A_{mj}^{[2]} = \mathrm{Tr}\, \mathbf{A}[\mathbf{O}_m, [\mathbf{O}_j, \mathbf{D}]_\mathrm{S}]_\mathrm{S} \tag{55}$$

$$\begin{aligned}\frac{\partial E_{mn}^{[2]}}{\partial X_j} \Rightarrow E_{mnj}^{[3]} = &-\mathrm{Tr}\, \mathbf{F}[[\mathbf{O}_n, [\mathbf{O}_j, \mathbf{D}]_\mathrm{S}], \mathbf{O}_m^\dagger]_\mathrm{S} - \\ &\mathrm{Tr}\, \mathbf{G}([\mathbf{O}_j, \mathbf{D}]_\mathrm{S})[[\mathbf{O}_n, \mathbf{D}]_\mathrm{S}, \mathbf{O}_m^\dagger]_\mathrm{S} - \\ &\mathrm{Tr}\, \mathbf{G}([\mathbf{O}_n, \mathbf{D}]_\mathrm{S})[[\mathbf{O}_j, \mathbf{D}]_\mathrm{S}, \mathbf{O}_m^\dagger]_\mathrm{S} - \\ &\mathrm{Tr}\, \mathbf{G}([\mathbf{O}_n, [\mathbf{O}_j, \mathbf{D}]_\mathrm{S}]_\mathrm{S})[\mathbf{D}, \mathbf{O}_m^\dagger]_\mathrm{S} - \\ &\mathrm{Tr}\, \mathbf{T}^{\mathrm{xc}}([\mathbf{O}_n, \mathbf{D}]_\mathrm{S},\ [\mathbf{O}_j, \mathbf{D}]_\mathrm{S})[\mathbf{D}, \mathbf{O}_m^\dagger]_\mathrm{S}\end{aligned} \tag{56}$$

$$\frac{\partial S_{mn}^{[2]}}{\partial X_j} \Rightarrow S_{mnj}^{[3]} = -\mathrm{Tr}\, \mathbf{O}_m^\dagger \mathbf{S}[\mathbf{O}_n, [\mathbf{D}, \mathbf{O}_j]_\mathrm{S}]_\mathrm{S}\mathbf{S} \tag{57}$$

where we have taken advantage of the rule

$$\frac{\partial \mathbf{D}}{\partial X_j} = -[\mathbf{O}_j, \mathbf{D}]_\mathrm{S} \tag{58}$$

which stems from the exponential parametrization of the density, and introduced the matrix $\mathbf{T}^{\mathrm{xc}}$[41]

$$T_{\mu\nu}^{\mathrm{xc}}(\mathbf{N}, \mathbf{M}) = \sum_{\rho\sigma\eta\varepsilon} M_{\sigma\rho} N_{\varepsilon\eta} \int \Omega_{\eta\varepsilon}(\mathbf{t})\, \Omega_{\rho\sigma}(\mathbf{s})\, \Omega_{\mu\nu}(\mathbf{r}) \frac{\delta^2 v_{\mathrm{xc}}(\mathbf{r})}{\delta\rho(\mathbf{s})\, \delta\rho(\mathbf{t})} \mathrm{d}\mathbf{r}\, \mathrm{d}\mathbf{s}\, \mathrm{d}\mathbf{t} \tag{59}$$

Using the differentiated matrices introduced above allows us to rewrite eqs 41d, 43e, and 52d, in the form

$$\bar{X}_m^* E_{mj}^{[2]} = \eta_j^*; \qquad \bar{\boldsymbol{X}}^\dagger \boldsymbol{E}^{[2]} = \boldsymbol{\eta}^\dagger \tag{60}$$

where the explicit values of the elements of the right-hand-side vector (matrix) $\boldsymbol{\eta}^\dagger$ vary according to the property we are differentiating. For the linear-response-function derivative, we get

$$\eta_j^* = -b_m^\omega A_{mj}^{[2]} + a_m^{\omega *} E_{mnj}^{[3]} b_n^\omega - \omega a_m^{\omega *} S_{mnj}^{[3]} b_n^\omega - a_m^{\omega *} B_{mj}^{[2]} \tag{61}$$

whereas for the residue (transition moment) derivative

$$\eta_j^* = b_m^f A_{mj}^{[2]} - a_m^{\omega_f *} E_{mnj}^{[3]} b_n^f + \omega_f (a_m^{\omega_f *} S_{mnj}^{[3]} b_n^{f*}) - \bar{\omega}(b_m^{f*} S_{mnj}^{[3]} b_n^f) \tag{62}$$

with $\bar{\omega}$ as in eq 45. Finally, for the excitation energy derivative

$$\eta_j^* = b_m^{f*} E_{mnj}^{[3]} b_n^f - \omega_f (b_m^{f*} S_{mnj}^{[3]} b_n^f) \tag{63}$$

where $\partial E_0 / \partial X_j = 0$ because it corresponds to the optimization condition, eq 16. As previously done for the $\bar{\boldsymbol{\lambda}}$, we recast the equation in the adjoint form

$$\boldsymbol{E}^{[2]} \bar{\boldsymbol{X}} = \boldsymbol{\eta} \tag{64}$$

and solve it by reusing the iterative, linear-scaling, response solver (with transformation on the right index) of ref 34 with a modified right-hand-side matrix.

2.6. The Generalized Property Gradient with Respect to Displacements of the Nuclei. Once all of the parameters and Lagrange multipliers have been determined, we can turn our attention to the third-order properties, which are obtained as derivatives of the Lagrangians with respect to displacements of the nuclei, as indicated in eq 36. The final geometric derivative of the linear response function reads

$$\frac{\mathrm{d}\mathcal{C}}{\mathrm{d}R_\beta} = -\frac{\partial A_m^{[1]}}{\partial R_\beta} b_m^\omega + a_m^{\omega *} \frac{\partial E_{mn}^{[2]}}{\partial R_\beta} b_n^\omega - \omega a_m^{\omega *} \frac{\partial S_{mn}^{[2]}}{\partial R_\beta} b_n^\omega - a_m^{\omega *} \frac{\partial B_m^{[1]}}{\partial R_\beta} - \bar{X}_m^* \frac{\partial E_m^{[1]}}{\partial R_\beta} \quad (65)$$

The transition moment gradient is

$$\frac{\mathrm{d}\mathcal{C}}{\mathrm{d}R_\beta} = \frac{\partial A_m^{[1]}}{\partial R_\beta} b_m^f - \frac{1}{2}(A_l^{[1]} b_l^f) b_m^{f*} \frac{\partial S_{mn}^{[2]}}{\partial R_\beta} b_n^f - a_m^{\omega_f *} \left(\frac{\partial E_{mn}^{[2]}}{\partial R_\beta} - \omega_f \frac{\partial S_{mn}^{[2]}}{\partial R_\beta} - \frac{\partial \omega_f}{\partial R_\beta} S_{mn}^{[2]} \right) b_n^f - \bar{X}_m^* \frac{\partial E_m^{[1]}}{\partial R_\beta} \quad (66)$$

where

$$\frac{\partial \omega_f}{\partial R_\beta} = b_m^{f*} \frac{\partial E_{mn}^{[2]}}{\partial R_\beta} b_n^f - \omega_f b_m^{f*} \frac{\partial S_{mn}^{[2]}}{\partial R_\beta} b_n^f \quad (67)$$

Note, however, the term including $\partial\omega_f/\partial R_\beta$ in the residue gradient vanishes since $a_m^{\omega_f *} S_{mn}^{[2]} b_n^f = 0$. This is due to the fact that $\boldsymbol{a}^{\omega_f}$ fulfills the projection relation $\boldsymbol{a}^{\omega_f} = \boldsymbol{P}_f(\boldsymbol{a}^{\omega_f})$, which removes all $\boldsymbol{b}^f$ components from the linear response vector.

Finally, for the excited-state gradient

$$\frac{d\mathcal{C}}{dR_\beta} = \frac{\partial E_0}{\partial R_\beta} + b_m^{f*} \frac{\partial E_{mn}^{[2]}}{\partial R_\beta} b_n^f - \omega_f b_m^{f*} \frac{\partial S_{mn}^{[2]}}{\partial R_\beta} b_n^f - \bar{X}_m^* \frac{\partial E_m^{[1]}}{\partial R_\beta} \quad (68)$$

2.7. Implementation. At variance with respect to what is required in standard linear and quadratic response calculations,[34,41,42] we need to implement the right-hand-side matrices $\boldsymbol{\eta}$ for the (adjoint) Lagrangian multiplier equations, as well as the final gradient expressions.

Comparing the expressions in eqs 61, 62, and 63, we write—in a somewhat self-explanatory notation—

$$\boldsymbol{\eta} = \boldsymbol{\eta}^{E3} + \boldsymbol{\eta}^{S3} + \boldsymbol{\eta}^{A2} + \boldsymbol{\eta}^{B2} \quad (69)$$

where it is understood that the contribution $\boldsymbol{\eta}^{B2} = \mathbf{0}$ in the transition moment case, and $\boldsymbol{\eta}^{A2} = \boldsymbol{\eta}^{B2} = \mathbf{0}$ for the excited state.

The explicit expressions for the four contributions are found as

$$\boldsymbol{\eta}^{B2} = [[\mathbf{S}, \mathbf{B}^\dagger]_\mathrm{a}, \mathbf{S}]_\mathrm{D} \quad (70)$$

$$\boldsymbol{\eta}^{A2} = -[[\mathbf{S}, \mathbf{A}]_\mathrm{b}, \mathbf{S}]_\mathrm{D} \quad (71)$$

$$\boldsymbol{\eta}^{S3} = \mathbf{S}[\mathbf{D}, [\mathbf{a}, \mathbf{b}^\dagger]_\mathrm{S}]_\mathrm{S}\mathbf{S} = \mathbf{0} \quad (72)$$

$$\boldsymbol{\eta}^{E3} = \mathbf{CDS} - \mathbf{SDC} \quad (73)$$

with

$$\mathbf{C} = [\mathbf{S}, [\mathbf{F}, \mathbf{S}]_\mathrm{a}]_{\mathrm{b}^\dagger} + [\mathbf{S}, \mathbf{G}([\mathbf{a}, \mathbf{D}]_\mathrm{S})]_{\mathrm{b}^\dagger} + [\mathbf{S}, \mathbf{G}([\mathbf{b}^\dagger, \mathbf{D}]_\mathrm{S})]_\mathrm{a} + \mathbf{G}([[\mathbf{b}^\dagger, \mathbf{D}]_\mathrm{S}, \mathbf{a}]_\mathrm{S}) + \mathbf{T}^{\mathrm{xc}}([\mathbf{b}^\dagger, \mathbf{D}]_\mathrm{S}, [\mathbf{a}, \mathbf{D}]_\mathrm{S}) \quad (74)$$

Above, **a** and **b** indicate, respectively, the linear response matrices for the *A* and *B* operators in the case of the linear response function; the *projected* linear response matrix at $\omega = \omega_f$, $\mathbf{a}^{\omega_f}$, and the eigenvector matrix $\mathbf{b}^f$ for the transition moment; and the excitation vector and its adjoint for the excited state gradient. Note that all $\boldsymbol{S}^{[3]}$ contributions actually vanish, as shown in Appendix A. This also applies for the additional contribution to the right-hand side originating from the last term in eq 62 in the case of the transition moment derivative

$$\bar{\omega}\mathbf{S}[\mathbf{D}, [\mathbf{b}^f, \mathbf{b}^{f\dagger}]_\mathrm{S}]_\mathrm{S}\mathbf{S} = \mathbf{0} \quad (75)$$

For the final computational expressions of the property gradients, we need, in addition to the undifferentiated density, Fock and overlap matrices at the expansion point $\mathbf{R}_0$ and the integral matrices **A** and **B**, the differentiated one- and two-electron integral matrices $\mathbf{h}^{R_\beta}$ and $\mathbf{G}^{R_\beta}$, the differentiated overlap matrices $\mathbf{S}^{R_\beta}$, and the differentiated integral matrices $\mathbf{A}^{R_\beta}$ and $\mathbf{B}^{R_\beta}$, since we are considering a perturbation-dependent basis set where each atomic orbital is centered on a specific atom and thus depends on the spatial coordinates of the nuclei. Explicit expressions for the matrix elements of $\mathbf{A}^{R_\beta}$, when *A* is the dipole moment operator, can be found in ref 44.

In ref 40, the derivatives of the individual matrices in the AO formulation were considered. It was there shown that the first derivative of the density, $\mathbf{D}^{R_\beta}(\mathbf{X})$, is given by the first derivative of the reference density matrix, $\mathbf{D}^{R_\beta}$, which, from the idempotency condition for **D**, is found to be

$$\mathbf{D}^{R_\beta} = -\mathbf{D}\mathbf{S}^{R_\beta}\mathbf{D} \quad (76)$$

Comparing the three Lagrangian expressions in eqs 37, 38, and 39, we can thus write (once again in a self-explanatory notation)

$$\mathcal{L}^{A1} = A_m^{[1]} b_m = -\mathrm{Tr}\,\mathbf{A}[\mathbf{b}, \mathbf{D}]_\mathrm{S} \quad (77)$$

$$\mathscr{L}^{B1} = a_m^* B_m^{[1]} = \mathrm{Tr}\,\mathbf{B}[\mathbf{D}, \mathbf{a}^\dagger]_S \tag{78}$$

$$\mathscr{L}^{E1} = \bar{X}_m^* E_m^{[1]} = \mathrm{Tr}\,\mathbf{F}[\mathbf{D}, \bar{\mathbf{X}}^\dagger]_S \tag{79}$$

$$\mathscr{L}^{E2} = a_m^* E_{mn}^{[2]} b_n = \mathrm{Tr}\,\mathbf{F}[[\mathbf{b}, \mathbf{D}]_S, \mathbf{a}^\dagger]_S + \mathrm{Tr}\,\mathbf{G}([\mathbf{b}, \mathbf{D}]_S)[\mathbf{D}, \mathbf{a}^\dagger]_S \tag{80}$$

$$\mathscr{L}^{S2} = a_m^* S_{mn}^{[2]} b_n = \mathrm{Tr}\,\mathbf{a}^\dagger \mathbf{S}[\mathbf{D}, \mathbf{b}]_S \mathbf{S} \equiv -\mathrm{Tr}\,\mathbf{a}^\dagger \mathbf{S}[\mathbf{b}, \mathbf{D}]_S \mathbf{S} \tag{81}$$

When the perturbed densities

$$\mathbf{D}^b = [\mathbf{b}, \mathbf{D}]_S \tag{82}$$

$$\mathbf{D}^{b,R_\beta} = [\mathbf{b}, \mathbf{D}^{R_\beta}]_S + [\mathbf{b}, \mathbf{D}]_{S^{R_\beta}} \tag{83}$$

are introduced, the geometric derivatives of the above individual contributions can be written

$$\frac{\partial \mathscr{L}^{A1}}{\partial R_\beta} = \mathrm{Tr}\{\mathbf{b}([\mathbf{A}^{R_\beta}, \mathbf{S}]_D + [\mathbf{A}, \mathbf{S}^{R_\beta}]_D + [\mathbf{A}, \mathbf{S}]_{D^{R_\beta}})\} \tag{84}$$

$$\frac{\partial \mathscr{L}^{B1}}{\partial R_\beta} = \mathrm{Tr}\{\mathbf{a}^\dagger([\mathbf{B}^{R_\beta}, \mathbf{S}]_D + [\mathbf{B}, \mathbf{S}^{R_\beta}]_D + [\mathbf{B}, \mathbf{S}]_{D^{R_\beta}})\} \tag{85}$$

$$\frac{\partial \mathscr{L}^{S2}}{\partial R_\beta} = -\mathrm{Tr}\{\mathbf{a}^\dagger(\mathbf{S}^{R_\beta}\mathbf{D}^b\mathbf{S} + \mathbf{S}\mathbf{D}^{b,R_\beta}\mathbf{S} + \mathbf{S}\mathbf{D}^b\mathbf{S}^{R_\beta})\} \tag{86}$$

$$\begin{aligned}\frac{\partial \mathscr{L}^{E1}}{\partial R_\beta} &= \mathrm{Tr}\{\bar{\mathbf{X}}^\dagger([\mathbf{F}^{R_\beta}, \mathbf{S}]_D + [\mathbf{F}, \mathbf{S}^{R_\beta}]_D + [\mathbf{F}, \mathbf{S}]_{D^{R_\beta}})\} + \mathrm{Tr}\{\mathbf{G}(\mathbf{D}^{R_\beta})[\mathbf{D}, \bar{\mathbf{X}}^\dagger]_S\} = \\ &\mathrm{Tr}\{\bar{\mathbf{X}}^\dagger([\mathbf{F}^{R_\beta}, \mathbf{S}]_D + [\mathbf{F}, \mathbf{S}^{R_\beta}]_D + [\mathbf{F}, \mathbf{S}]_{D^{R_\beta}})\} + \mathrm{Tr}\{\mathbf{G}([\mathbf{D}, \bar{\mathbf{X}}^\dagger]_S)\mathbf{D}^{R_\beta}\}\end{aligned} \tag{87}$$

$$\begin{aligned}\frac{\partial \mathscr{L}^{E2}}{\partial R_\beta} &= \mathrm{Tr}\{\mathbf{F}^{R_\beta}[\mathbf{D}^b, \mathbf{a}^\dagger]_S + \mathbf{F}[\mathbf{D}^{b,R_\beta}, \mathbf{a}^\dagger]_S + \mathbf{F}[\mathbf{D}^b, \mathbf{a}^\dagger]_{S^{R_\beta}} + \\ &\mathbf{G}(\mathbf{D}^{R_\beta})[\mathbf{D}^b, \mathbf{a}^\dagger]_S\} + \mathrm{Tr}\{\mathbf{G}^{R_\beta}(\mathbf{D}^b)[\mathbf{D}, \mathbf{a}^\dagger]_S + \\ &\mathbf{G}(\mathbf{D}^{b,R_\beta})[\mathbf{D}, \mathbf{a}^\dagger]_S + \mathbf{G}(\mathbf{D}^b)[\mathbf{D}^{R_\beta}, \mathbf{a}^\dagger]_S + \mathbf{G}(\mathbf{D}^b)[\mathbf{D}, \mathbf{a}^\dagger]_{S^{R_\beta}}\} = \\ &\mathrm{Tr}\{\mathbf{F}^{R_\beta}[\mathbf{D}^b, \mathbf{a}^\dagger]_S + \mathbf{F}[\mathbf{D}^{b,R_\beta}, \mathbf{a}^\dagger]_S + \mathbf{F}[\mathbf{D}^b, \mathbf{a}^\dagger]_{S^{R_\beta}} + \\ &\mathbf{G}([\mathbf{D}^b, \mathbf{a}^\dagger]_S)\mathbf{D}^{R_\beta}\} + \mathrm{Tr}\{\mathbf{G}^{R_\beta}(\mathbf{D}^b)[\mathbf{D}, \mathbf{a}^\dagger]_S + \\ &\mathbf{G}([\mathbf{D}, \mathbf{a}^\dagger]_S)\mathbf{D}^{b,R_\beta} + \mathbf{G}(\mathbf{D}^b)[\mathbf{D}^{R_\beta}, \mathbf{a}^\dagger]_S + \mathbf{G}(\mathbf{D}^b)[\mathbf{D}, \mathbf{a}^\dagger]_{S^{R_\beta}}\}\end{aligned} \tag{88}$$

where we take advantage of the fact that $\mathrm{Tr}\{\mathbf{G}(\mathbf{M})\mathbf{N}\} = \mathrm{Tr}\{\mathbf{G}(\mathbf{N})\mathbf{M}\}$ (and similarly for the differentiated $\mathrm{Tr}\{\mathbf{G}^{R_\beta}(\mathbf{M})\mathbf{N}\}$) to avoid computing two-electron Fock matrices for R-perturbed matrices, since it would require $3N$ Fock matrices computations.

Introducing the derivatives 84−88 into the generalized property expressions, eqs 65, 66, and 68, the explicit computational expressions for the property gradients are obtained, with the appropriate linear response matrices and eigenvector matrices taking the place of the generic $\mathbf{a}^\dagger$ and $\mathbf{b}$ matrices. For instance, the final computational expression for the linear-response function gradient reads

$$\begin{aligned}\frac{d\mathscr{O}}{dR_\beta} &= -\mathrm{Tr}\{\mathbf{b}([\mathbf{A}^{R_\beta}, \mathbf{S}]_D + [\mathbf{A}, \mathbf{S}^{R_\beta}]_D + [\mathbf{A}, \mathbf{S}]_{D^{R_\beta}})\} - \\ &\mathrm{Tr}\{\mathbf{a}^\dagger([\mathbf{B}^{R_\beta}, \mathbf{S}]_D + [\mathbf{B}, \mathbf{S}^{R_\beta}]_D + [\mathbf{B}, \mathbf{S}]_{D^{R_\beta}})\} + \\ &\mathrm{Tr}\{\mathbf{F}^{R_\beta}[\mathbf{D}^b, \mathbf{a}^\dagger]_S + \mathbf{F}[\mathbf{D}^{b,R_\beta}, \mathbf{a}^\dagger]_S + \mathbf{F}[\mathbf{D}^b, \mathbf{a}^\dagger]_{S^{R_\beta}} + \\ &\mathbf{G}([\mathbf{D}^b, \mathbf{a}^\dagger]_S)\mathbf{D}^{R_\beta}\} + \mathrm{Tr}\{\mathbf{G}^{R_\beta}(\mathbf{D}^b)[\mathbf{D}, \mathbf{a}^\dagger]_S + \\ &\mathbf{G}([\mathbf{D}, \mathbf{a}^\dagger]_S)\mathbf{D}^{b,R_\beta} + \mathbf{G}(\mathbf{D}^b)([\mathbf{D}^{R_\beta}, \mathbf{a}^\dagger]_S + [\mathbf{D}, \mathbf{a}^\dagger]_{S^{R_\beta}})\} + \\ &\omega\,\mathrm{Tr}\{\mathbf{a}^\dagger(\mathbf{S}^{R_\beta}\mathbf{D}^b\mathbf{S} + \mathbf{S}\mathbf{D}^{b,R_\beta}\mathbf{S} + \mathbf{S}\mathbf{D}^b\mathbf{S}^{R_\beta})\} - \\ &\mathrm{Tr}\{\bar{\mathbf{X}}^\dagger\{[\mathbf{F}^{R_\beta}, \mathbf{S}]_D + [\mathbf{F}, \mathbf{S}^{R_\beta}]_D + [\mathbf{F}, \mathbf{S}]_{D^{R_\beta}}\}\} - \\ &\mathrm{Tr}\{\mathbf{G}([\mathbf{D}, \bar{\mathbf{X}}^\dagger]_S)\mathbf{D}^{R_\beta}\}\end{aligned} \tag{89}$$

with $\mathbf{a}^\dagger = \mathbf{a}^{\omega\dagger}$ and $\mathbf{b} = \mathbf{b}^\omega$.

The expression for the transition moment gradient is straightforwardly obtained from eq 89 by removing all terms involving the property integral matrix $\mathbf{B}$ and its geometric derivative $\mathbf{B}^R$, adding the $(\partial \mathscr{L}^{S2})/(\partial R_\beta)$ term multiplied by $\bar{\omega}$, with

$$\bar{\omega} = \frac{1}{2}\mathrm{Tr}\{\mathbf{A}[\mathbf{D}, \mathbf{b}^f]_S\} \tag{90}$$

and using ω_f instead of ω as factor in the third-last term. In this case, $\mathbf{a}^\dagger = \mathbf{a}^{\omega_f\dagger}$ and $\mathbf{b} = \mathbf{b}^f$.

In the excited state gradient, the terms involving the integral matrix $\mathbf{A}$ and its geometric derivative $\mathbf{A}^{R_\beta}$ also disappear and are replaced by the computational expression of the ground-state energy gradient[40]

$$\frac{\partial E_0}{\partial R_\beta} = \mathrm{Tr}\,\mathbf{D}\mathbf{h}^{R_\beta} + \frac{1}{2}\mathrm{Tr}\,\mathbf{D}\mathbf{G}^{R_\beta}(\mathbf{D}) + \mathrm{Tr}\,\mathbf{D}^{R_\beta}\mathbf{F} + h_{\mathrm{nuc}}^{R_\beta} \tag{91}$$

again with ω_f as the factor on the analog of the third-last term of eq 89, and with $\mathbf{a}^\dagger = \mathbf{b}^{f,\dagger}$ and $\mathbf{b} = \mathbf{b}^f$.

Note also that in Kohn−Sham theory the exchange-correlation contribution to the matrix $\mathbf{G}^{R_\beta}(\mathbf{D}^b)$ has a rather complicated expression, which is explicitly given in Appendix B.5.

If we replace the differentiated Hamilton operator (matrices) with a generic one-electron operator, C, in the above-given gradients, it is easy to prove that the computational expressions for the standard quadratic response function $\langle\langle A; B, C\rangle\rangle_{\omega,0}$ and its single and double residues are obtained. The proof is given in detail in section 2.4.2 of ref 28, starting from the expressions for the linear response function and transition moment magnetic gradients on LAOs, which, as mentioned in the Introduction, bear strong similarities with the gradients here considered.

As an addition to the discussion in ref 28, we report here the computational expression of a generic excited-state first-order property (component)—like for instance the excited state molecular electric dipole moment—as straightforwardly obtained from the excited-state gradient computational expression:

$$C_\alpha^f = \langle f|C_\alpha|f\rangle = \mathrm{Tr}\,\mathbf{D}\mathbf{C}_\alpha + C_{\alpha,\mathrm{nuc}} - \mathrm{Tr}\{[[\mathbf{b}^f, \mathbf{D}]_S, \mathbf{b}^{f\dagger}]_S - [\mathbf{D}, \bar{\mathbf{X}}^\dagger]_S\}\mathbf{C}_\alpha \tag{92}$$

The first two terms in eq 92 correspond to the ground-state first-order property. It is well-known that excited-state first-order properties can also be computed as double residues of the quadratic response function.[42]

Also, the geometric gradient of any ground-state first-order property can be immediately obtained from the ground-state energy gradient in eq 91,

$$\frac{\partial C_\alpha}{\partial R_\beta} = \mathrm{Tr}\,\mathbf{D}\mathbf{C}_\alpha^{R_\beta} + \mathrm{Tr}\,\mathbf{D}^{R_\beta}\mathbf{C}_\alpha + C_{\alpha,\mathrm{nuc}}^{R_\beta} \tag{93}$$

3. Illustrative Results

The calculation of the geometric gradients of the linear response function, of its poles, and of its residues has been implemented within the linear-scaling development version of the Dalton code[34,45,46] at the Hartree−Fock and DFT levels of theory. The approach is general and encompasses the geometric gradient of any molecular property that can be related to the linear response function and its residues, like, for instance, the electric-dipole polarizability $\alpha_{\alpha\beta}(-\omega;\omega)$, whose geometric gradient is a key ingredient in the computational simulation of spectroscopic effects like Raman scattering[10] and coherent anti-Stokes Raman scattering.[11]

Various implementations of the polarizability as well as of the excited-state gradient have appeared in recent years, see for example refs 9, 11, and 23, whereas no analytic implementation of the electronic transition dipole moment derivative in a DFT framework has been presented. Note, however, an earlier CASSCF-based implementation of analytic derivatives of $\boldsymbol{\mu}_{kl}$ reported in ref 39. For this reason, as a specific illustrative application of the implementation, we will present and discuss here the results of a hybrid-functional DFT study of the vibronic fine structure of the $\tilde{X}(^1A_{1g}) - \tilde{A}(^1B_{2u})$ transition in the absorption spectrum of benzene. In the electric dipole approximation, this transition is Franck−Condon-forbidden and hence basically determined by the (first-order) Herzberg−Teller integrals and electronic transition dipole-moment derivatives. For such a study, the gradients of both the poles and residues have been used.

3.1. Herzberg−Teller Contribution to One-Photon (UV) Spectra. Quantum mechanical rovibronic transition moments, to which approximations are numerically calculated herein, are directly related to the experimentally determined integrated line strength of a rovibronic transition. Following ref 47, the integrated net absorption cross-section G_{net} reads

$$G_{\mathrm{net}} = \int_{\tilde{\nu}_1}^{\tilde{\nu}_2} \sigma_{\mathrm{net}}(\tilde{\nu})\tilde{\nu}^{-1}\,\mathrm{d}\tilde{\nu} = \int_{\tilde{\nu}_1}^{\tilde{\nu}_2} \sigma_{\mathrm{net}}(\tilde{\nu})\,\mathrm{d}\ln\tilde{\nu} \tag{94}$$

and thus depends on the wavenumber $\tilde{\nu}$-dependent absorption cross-section $\sigma_{\mathrm{net}}(\tilde{\nu})$, which is logarithmically integrated (see, e.g., ref 48 for a discussion) over a suitably chosen wavenumber interval that includes the entire absorption band.[47] The net absorption cross-section $\sigma_{\mathrm{net}}(\tilde{\nu})$ of a one-photon transition is connected via the Lambert−Beer law to the ratio between transmitted and incident spectral intensity $I_{\mathrm{tr},\tilde{\nu}}(\tilde{\nu})$ and $I_{0,\tilde{\nu}}(\tilde{\nu})$, respectively, (see ref 47 for a rigorous definition of these terms)

$$\sigma_{\mathrm{net}}(\tilde{\nu}) = \frac{1}{N_{\mathrm{A}}cl}\ln\left[\frac{I_{\mathrm{tr},\tilde{\nu}}(\tilde{\nu})}{I_{0,\tilde{\nu}}(\tilde{\nu})}\right] = \frac{A_{\mathrm{e}}(\tilde{\nu})}{N_{\mathrm{A}}cl} = \frac{\varepsilon(\tilde{\nu})\ln(10)}{N_{\mathrm{A}}} \tag{95}$$

where N_{A} is the Avogadro number, c the amount of substance concentration of the absorbing species, l the path length through the absorbing material, A_{e} the (Naperian) absorbance, and $\epsilon(\tilde{\nu})$ the molar (decadic) absorption coefficient. When stimulated emission can be neglected, the net integrated absorption cross-section between two energy levels is composed of the line strengths of the underlying individual transition processes between states i and j, which are summed over and weighted according to the (fractional) population p_i of the corresponding initial state:[47]

$$G_{\mathrm{net}} = \sum_{i,j} p_i G_{ij} \tag{96}$$

The individual integrated absorption cross-section is, via $G_{ij} = hB_{\tilde{\nu},ij}$, related to the Einstein coefficient $B_{\tilde{\nu},ij}$ for absorption and thus directly connected to the quantum mechanical transition moment. For the electric dipole transitions considered herein, the relation between electric transition dipole moment $\boldsymbol{M}_{ij}$ and integrated band strength G_{ij} is[47]

$$G_{ij} = \frac{8\pi^3}{(4\pi\varepsilon_0)3hc_0}|\boldsymbol{M}_{ij}|^2 \tag{97}$$

with $|\boldsymbol{M}_{ij}|^2 = \sum_\alpha |\langle i|\hat{\mu}_\alpha|j\rangle|^2$ and $\alpha = x,\ y,\ z$. In contrast to the oscillator strength f, which is frequently used in UV/vis absorption spectroscopy, the integrated absorption band strength does not explicitly depend on the transition wavenumber. When f_{ij} is defined as[47]

$$f_{ij} \approx \frac{m_{\mathrm{e}}c_0 8\pi^2\tilde{\nu}_{ij}}{e^2 3h}|\boldsymbol{M}_{ij}|^2 = \frac{(4\pi\varepsilon_0)m_{\mathrm{e}}c_0^2\tilde{\nu}_{ij}}{\pi e^2}G_{ij} \tag{98}$$

one obtains the following approximate relationship between oscillator strength and integrated band strength, which has been employed herein to convert previously reported values for f_{ij} (or f) to integrated band strengths G_{ij} (or G_{net}):

$$f_{ij} \approx 1.1295835 \times 10^{-8}(\tilde{\nu}_{ij}/\mathrm{cm}^{-1})(G_{ij}/\mathrm{pm}^2);$$
$$f \approx 1.1295835 \times 10^{-8}(\tilde{\nu}_0/\mathrm{cm}^{-1})(G_{\mathrm{net}}/\mathrm{pm}^2) \tag{99}$$

with $\tilde{\nu}_0$ denoting the transition wavenumber of the corresponding band center.

The electric transition dipole moment $\boldsymbol{M}_{\kappa\lambda}$ between two rovibronic states characterized by the rovibronic wave functions $\Psi_\kappa(\mathbf{r},\mathbf{R})$ and $\Psi_\lambda(\mathbf{r},\mathbf{R})$, which depend on the collective electronic spatial coordinates $\mathbf{r}$ and the collective spatial coordinates $\mathbf{R}$ of the nuclei, is, in the adiabatic approximation, given by

$$\boldsymbol{M}_{\kappa\lambda} = \langle\kappa|\boldsymbol{\mu}|\lambda\rangle \approx \langle\kappa_k|\langle k|\boldsymbol{\mu}|l\rangle|\lambda_l\rangle = \langle\kappa_k|\boldsymbol{\mu}_{kl}|\lambda_l\rangle = \boldsymbol{M}_{\kappa k\lambda l} \tag{100}$$

with the adiabatic electronic wave functions $\psi_k(\mathbf{r};\mathbf{R})$ and $\psi_l(\mathbf{r};\mathbf{R})$ depending explicitly on the spatial coordinates of the electrons and parametrically on the spatial coordinates of the nuclei. The wave functions $\chi_{\kappa,k}(\mathbf{R})$ and $\chi_{\lambda,l}(\mathbf{R})$ for the

motion of the nuclei depend, like the electronic transition dipole moment $\mu_{kl}(\mathbf{R})$, only on the coordinates of the various nuclei.

If a Taylor series expansion is applied to $\boldsymbol{\mu}_{kl}(\mathbf{R})$, for instance around the equilibrium molecular structure $\mathbf{R}_0$ of the initial electronic state, the expansion yields

$$\boldsymbol{\mu}_{kl}(\mathbf{R}) = \boldsymbol{\mu}_{kl}(\mathbf{R}_0) + \sum_{\beta} \left.\frac{\partial \boldsymbol{\mu}_{kl}(\mathbf{R})}{\partial R_\beta}\right|_{\mathbf{R}=\mathbf{R}_0} (R_\beta - R_{0,\beta}) + \ldots \tag{101}$$

By inserting this expansion into eq 100, the electric transition dipole moment is expressed as a sum of Franck−Condon and Herzberg−Teller contributions corresponding to the terms involving the electronic transition dipole moment and the first derivative of the electronic transition dipole moment with respect to displacements of the nuclei computed at the molecular equilibrium structure, respectively, in addition to higher-order terms. If the latter are neglected, one obtains

$$\boldsymbol{M}_{kk\lambda l} = \boldsymbol{\mu}_{kl}(\mathbf{R}_0)\langle\kappa_k|\lambda_l\rangle + \sum_{\beta} \left.\frac{\partial \boldsymbol{\mu}_{kl}(\mathbf{R})}{\partial R_\beta}\right|_{\mathbf{R}=\mathbf{R}_0} \langle\kappa_k|(\hat{R}_\beta - \hat{R}_{0,\beta})|\lambda_l\rangle \tag{102}$$

Within the Born−Oppenheimer adiabatic approximation, which is employed in this work, the transition dipole moment and its first derivatives with respect to nuclear displacements can be computed analytically using the DFT-based framework developed in this paper. We note in passing that, in addition to the Herzberg−Teller terms, terms arising through diabatic (frequently called nonadiabatic) coupling also contribute to the transition dipole moment[49] to this order, which are, however, neglected in the present study.

Franck−Condon integrals $\langle\kappa_k|\lambda_l\rangle$ and Herzberg−Teller integrals $\langle\kappa_k|(\hat{R}_\beta - \hat{R}_{0,\beta})|\lambda_l\rangle$ involve the wave functions of the motions of the nuclei. If the vibrational motion is assumed to be harmonic and separable from the rotational and translational motion, the states $|\kappa_k\rangle$ and $|\lambda_l\rangle$ are expressed as direct products of multidimensional harmonic oscillator states $|v\rangle$ and $|v'\rangle$ (with quantum numbers v_i and v_i' for the various harmonic oscillators in the initial and final states, respectively) and corresponding rotational-translational states. The latter are not explicitly considered herein. To this end, the spatial coordinates of the nuclei $\mathbf{R}$ are replaced by the vibrational mass-weighted normal coordinates, denoted as $\mathbf{Q}$ and $\mathbf{Q}'$, in which the harmonic vibrational force fields of the two electronic states involved are diagonal, as well as by the Euler angles for rotation and by the spatial coordinates of the center of mass. Recently, a coherent state-based generating function approach for efficiently computing vibronic transition profiles within the Franck−Condon and Herzberg−Teller approximation (and beyond) has been outlined for Duschinsky rotated multidimensional harmonic oscillators at finite temperatures and at 0 K.[50] We employ this coherent state-based generating function approach implemented in the vibronic structure program hotFCHT,[13,51,52] which offers both a time-independent and time-dependent route to electric transition properties. The vibronic profile generating function $G_{\mathrm{FCHT}}(\mathbf{Z};\boldsymbol{\Lambda})$, not to be confused with the integrated band strengths G_{ij}, G_{net}, and G_{total}, consists of three parts: one containing the Franck−Condon factor, the second one the Franck−Condon/Herzberg−Teller integrals, and the last one the (first-order) Herzberg−Teller term,

$$\begin{aligned} G_{\mathrm{FCHT}}(\mathbf{Z};\boldsymbol{\Lambda}) = {} & |\boldsymbol{\mu}_{kl}(\mathbf{Q}_0)|^2 G^K_{\mathrm{FC}}(\mathbf{Z};\boldsymbol{\Lambda})^{(\hat{1},\hat{1})} + \\ & 2\sum_{\beta} \boldsymbol{\mu}_{kl}(\mathbf{Q}_0) \cdot \left(\frac{\partial \boldsymbol{\mu}_{kl}}{\partial Q_\beta}\right)_{\mathbf{Q}=\mathbf{Q}_0} G^K_{\mathrm{FC/HT}}(\mathbf{Z};\boldsymbol{\Lambda})^{(\hat{Q}_\beta,\hat{1})} + \\ & \sum_{\beta,\gamma} \left(\frac{\partial \boldsymbol{\mu}_{kl}}{\partial Q_\beta}\right)_{\mathbf{Q}=\mathbf{Q}_0} \cdot \left(\frac{\partial \boldsymbol{\mu}_{kl}}{\partial Q_\gamma}\right)_{\mathbf{Q}=\mathbf{Q}_0} G^K_{\mathrm{HT}}(\mathbf{Z};\boldsymbol{\Lambda})^{(\hat{Q}_\beta,\hat{Q}_\gamma)} \end{aligned} \tag{103}$$

where $\mathbf{Z}$ contains the generating function parameters, $\boldsymbol{\Lambda}$ is related to a thermal integration kernel K, $\hat{1}$ is the identity operator, and $\hat{Q}_\beta$ is the position operator corresponding to the βth normal coordinate Q_β. Details of the approach and the definition of the various terms in eq 103 can be located in ref 50.

3.2. Computational Details. As a test case, we present the results of calculations of the vibrational fine structure in the $\tilde{X}(^1A_{1g}) - \tilde{A}(^1B_{2u})$ one-photon UV absorption spectrum of benzene at 0 K. This transition is Franck−Condon-forbidden in the electric transition dipole approximation, that is, $\boldsymbol{\mu}_{kl}(\mathbf{Q_0}) = \mathbf{0}$ at the D_{6h} symmetric equilibrium structure of the initial and final electronic states, and becomes allowed due to Herzberg−Teller vibronic coupling. The time-dependent Hartree−Fock and the time-dependent density functional theory methods, the latter using the B3LYP functional[53,54] as well as its Coulomb attenuated variant camB3LYP,[55] were exploited for the electronic structure calculation within the linear-scaling development version of the Dalton program. As a basis set, the triple-ζ valence basis set with polarization functions (TZVP) of ref 56 was used. The grid employed is based on the original Becke partitioning and the radial grid of ref 57 multiplied by an angular Lebedev grid.[58−60] The grid is pruned for small R in order to avoid too many grid points with small weights, and the radial integration threshold was chosen to be 10^{-13}. The angular expansion order was chosen to be 42.

Equilibrium structures in the electronic ground state were obtained using analytic derivatives of the total electronic energy with respect to nuclear displacements using a convergence threshold of $10^{-5}\ E_h\ a_0^{-1}$ for the norm of the gradient and $10^{-4}\ E_h\ a_0^{-1}$ for its largest component. The total energy of each cycle was optimized to $10^{-6}\ E_h$. Harmonic force fields of the electronic ground state were calculated using analytic second derivatives with thresholds of 10^{-7} when solving the linear response equations. The equilibrium structures in the electronically excited state were computed using analytical derivatives of the excited-state energy with respect to displacements of the nuclei (see eq 68). The excitation energies were converged until changes remained below $10^{-6}\ E_h$, and the norm of the final excited state gradient was below $10^{-5}\ E_h\ a_0^{-1}$. The harmonic force constant matrix of the electronically excited states was computed using central numerical derivatives of analytic gradients of the electronic energy with respect to displacements of the nuclei. The finite size of the corresponding displacements was chosen as 0.01 a_0. The masses employed were those of the

Table 1. Harmonic Vibrational Wavenumbers (in cm^{-1}) for e_{2g} Modes of the $^1A_{1g}$ and $^1B_{2u}$ States of Benzene[a]

state	mode	B3LYP/ TZVP	camB3LYP/ TZVP	HF/ TZVP	CASSCF/ DZP[b]	exptl[c]
$^1A_{1g}$	ν_6	625	631/632	666	646	608
	ν_9	1202	1212	1284	1263	1178
	ν_8	1634	1673/1674	1771	1730	1600
	ν_7	3169	3196	3328	3369	3057
$^1B_{2u}$	ν_6'	533/539	538/539	563	575	521
	ν_9'	1181/1186	1192/1193	1265	1237	1148
	ν_8'	1565/1566	1606	1712	1665	1516
	ν_7'	3192/3194	3220	3356	3389	3077

[a] A pair of numbers separated by a slash is given when the vibrational wavenumbers for a pair of normal modes that are supposed to be degenerate are different due to numerical reasons (in the current work, we do not fully exploit point group symmetry). [b] Ref 13. [c] Taken from the compilation of data reported in ref 69.

most abundant isotopes (^{12}C,^1H). Electronic transition dipole moments (which vanish in the present case) and their analytic derivatives with respect to displacements of the nuclei were computed according to eq 66 at the computed equilibrium structures of the initial state. Symmetry has not been used when computing the electronic transition dipole moment derivatives, as well as the energy gradient and the harmonic force field in the electronically excited state. The other calculations were performed by taking advantage of the Abelian D_{2h} point group symmetry.

The plotted spectral profiles of the one-photon absorption spectra were determined within the more efficient time-dependent approach. In the evaluation of the Fourier transformation of the Lorentzian weighted time-correlation function (TCF), corresponding to the Lorentzian weighted eq 103 in the time domain, the FFTW[61] library (version 3.1.2) was used for the fast Fourier transformation with a grid size of 2^{15}, a time increment of $t \sim 1.0$ fs, and a time interval of (−16.384 ps, 16.384 ps). The real part of the Fourier transformed TCF was taken, and its norm was plotted after weighting with the transition wavenumber as the wavenumber-dependent absorption cross-section $\sigma(\tilde{\nu})$. Integrated absorption cross-sections of the individual vibronic transitions reported in the tables were directly computed within the time-independent framework.

3.3. Discussion of the Results. The computed harmonic vibrational wavenumbers of the modes which transform according to the irreducible representation e_{2g} (corresponding to ν_6, ν_7, ν_8, and ν_9 in the nomenclature of Wilson[62] and ν_{18}, ν_{15}, ν_{16}, and ν_{17} in the nomenclature of Herzberg, respectively) are reported in Table 1 for the electronic states $\tilde{X}(^1A_{1g})$ and $\tilde{A}(^1B_{2u})$. Only these doubly degenerate modes of benzene are capable of inducing intensity for this electric dipole transition via first-order Herzberg−Teller vibronic coupling, whereas in the second order, other modes such as e_{1g}, e_{1u}, and e_{2u} can act as inducing modes (see, e.g., ref 63). For comparison, we also report the experimental fundamental wavenumbers and the harmonic wavenumbers computed in ref 13 in the complete active space-self-consistent field (CASSCF) framework for the four e_{2g} modes.

The Herzberg−Teller absorption profiles computed for a temperature of 0 K on the basis of the results from the various electronic structure approaches are plotted in Figure 1. The

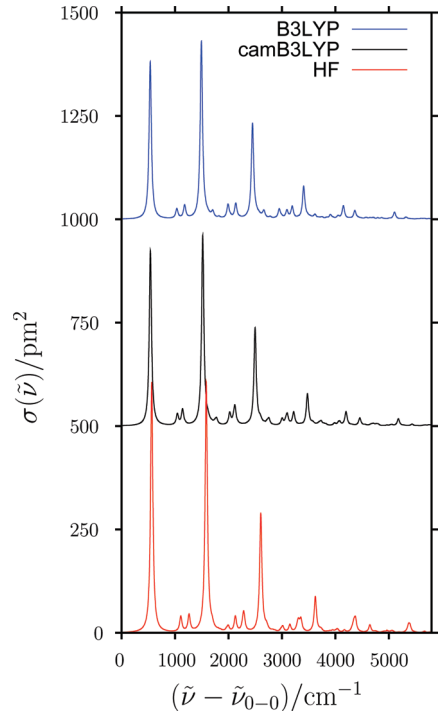

Figure 1. Calculated absorption cross-sections $\sigma(\tilde{\nu})$ (in pm^2) as a function of the wavenumber (in cm^{-1}) in excess of the 0−0 transition wavenumber $\tilde{\nu}_{0-0}$ as obtained from TDDFT (using the B3LYP and the camB3LYP functional) and from TDHF. Cross-sections were computed using the coherent state generating function approach in the time-dependent picture by exploiting the time-correlation function. For the graphical representation, the cross-sections computed with the B3LYP and camB3LYP hybrid density functionals were shifted by an increment of 1000 pm^2 and 500 pm^2, respectively. A Lorentzian line shape function with full-width at half-maximum of 50 cm^{-1} was employed, and the experimental value from ref 63 of $\tilde{\nu}_{0-0} = 38\,086$ cm^{-1} was used in converting the HT profile to wavenumber-dependent absorption cross-sections, which corresponds for an isolated band after logarithmic integration over a suitable wavenumber interval to the integrated absorption cross-section G of the vibronic band. The values of G reported in the tables were computed, however, directly in the time-independent picture via eqs 102 and 97.

0−0 transition in the $\tilde{X}(^1A_{1g}) - \tilde{A}(^1B_{2u})$ absorption spectrum of benzene is Franck−Condon-forbidden in the electric dipole approximation. The first vibronic band around $\tilde{\nu}_{0-0} + 550$ cm^{-1} serves as a so-called false origin brought about by the 6_0^1 transition (using Wilson's mode enumeration), on which the most prominent progression $6_0^1 1_0^{n'}$ builds, extending (visibly) up to about 5500 cm^{-1} above the 0−0 transition wavenumber. This progression is shortest (in terms of relative cross sections) at the Hartree−Fock level (abbreviated as HF below and in the tables) and longest for the B3LYP functional, which differs only slightly from the camB3LYP result. This finding is in line with the predicted change in the C−C bond length, for which HF gives only $\Delta r_{C-C} = 2.82$ pm, whereas B3LYP gives $\Delta r_{C-C} = 3.08$ pm and camB3LYP $\Delta r_{C-C} = 2.99$ pm. These C−C bond length elongations upon electronic excitation are significantly smaller than those predicted in ref 13 at the CASSCF level (3.8 pm), in ref.64 at the CCSD level (3.3 pm) and in ref 39

at the CASPT2 level (3.6 pm). This strongly impacts the overall shape of the progression in the breathing mode ν_1, which is predicted to be too short as compared to the multireference and coupled cluster methods, as well as the experiment. Less prominent progressions in this mode are built on the other false origins 7_0^1, 8_0^1, and 9_0^1 as well as on combination bands such as $6_0^1 16_0^2$ and $6_0^1 17_0^2$. For selected vibronic bands, we report in Table 2 the computed integrated absorption band strengths as well as their relative values and compare these to earlier computational results and experimental measurements. To facilitate this comparison, we have converted previously reported oscillator strengths to integrated (net) absorption band strengths using eq 99. When comparing experimental and theoretical band strengths, we do, however, not correct or account for temperature-dependent populations of the initial state, limited experimental resolutions, and other factors.

According to the Herzberg−Teller sum rule (see, e.g., ref 15), the total integrated absorption band strength G_{total} for the $\tilde{X}(^1A_{1g}) - \tilde{A}(^1B_{2u})$ transition of benzene at 0 K becomes in the harmonic approximation

$$G_{\text{total}} = \frac{8\pi^3}{(4\pi\varepsilon_0)3hc_0} \sum_{\beta} \frac{\hbar}{2\omega_\beta} \left| \left(\frac{\partial \boldsymbol{\mu}_{kl}}{\partial Q_\beta} \right)_{\mathbf{Q}=\mathbf{Q}_0} \right|^2 \qquad (104)$$

where ω_β is the harmonic frequency corresponding to the normal mode coordinate Q_β of the initial electronic state, and where the sum runs over all components of degenerate normal modes, including, for example, ν_{6a} and ν_{6b}. Alternatively, one weights the various terms with the degeneracies of the normal modes and sums over the contributions from the modes to obtain G_{total}. The total integrated cross-section can in this approximation be partitioned into contributions from each normal mode. Accordingly, the magnitude of the contribution of the various vibrational modes is determined by the harmonic frequency and the norm square of the first derivative of the electronic transition dipole moment. In Table 3, the contributions of the various e_{2g} vibrational modes to the integrated band strength from eq 104 as well as their sum are presented.

From Tables 2 and 3 it is evident that the ν_6 mode accounts for the major part of the first-order HT-induced absorption cross-section. One of the main differences between the

Table 2. Computed and Experimental Integrated Absorption Band Strengths (in pm^2) for Selected Vibronic Transitions between the Electronic Singlet Ground State ($^1A_{1g}$) and the Lowest Excited Singlet State ($^1B_{2u}$) of Benzene[a]

trans.	B3LYP/ TZVP	camB3LYP/ TZVP	HF/ TZVP	CASSCF/ DZP[b]	CASPT2/ ANO[c]	exp.[d]	exp.[e]	exp.[f]	exp.[g]	exp.[h]
6_0^1	0.784(1.00)	0.863(1.00)	1.232(1.00)	0.110(1.00)	0.205(1.00)	0.314(1.00)	0.20(1.00)	0.17(1.00)	(1.00)	(1.000)
$6_0^1 1_0^1$	0.861(1.10)	0.910(1.05)	1.199(0.97)	0.189(1.72)	0.309(1.50)	0.419(1.33)	0.338(1.68)	0.20(1.12)	(0.99)	(0.903)
$6_0^1 1_0^2$	0.448(0.57)	0.455(0.53)	0.554(0.45)	0.156(1.41)	0.220(1.07)	0.293(0.93)	0.287(1.42)	0.14(0.75)	(0.94)	(0.889)
$6_0^1 1_0^3$	0.147(0.19)	0.143(0.17)	0.162(0.13)	0.082(0.74)	0.099(0.48)	0.182(0.58)	0.15(0.72)	0.07(0.37)	(0.49)	(0.010)
$6_0^1 1_0^4$	0.034(0.04)	0.032(0.04)	0.033(0.03)	0.031(0.28)	0.031(0.15)	0.119(0.38)	0.07(0.36)	0.02(0.11)	(0.13)	
7_0^1	0.052(0.067)	0.058(0.067)	0.055(0.044)	0.006(0.054)	0.011(0.05)			0.01(0.07)	(0.06)	(0.034)
8_0^1	0.012(0.015)	0.008(0.008)	0.006(0.005)	0.004(0.033)	0.001(0.005)					(0.006)
9_0^1	0.005(0.007)	0.003(0.004)	0.0001(0.0001)	0.003(0.028)	0.008(0.04)				(0.02)	(0.018)

[a] Relative values for the integrated absorption cross-sections are reported in parentheses. [b] Values obtained using the same input data set as in ref 13. [c] Ref 39, oscillator strengths reported in ref 39 (for the CASPT2 equilibrium structures combined with CASSCF harmonic force fields and electronic transition dipole moments) were converted according to eq 99 using the reported computed transition wavenumbers. [d] Ref 67, oscillator strengths reported in ref 67 were converted according to eq 99 using the experimental transition wavelengths given in Table 1 of this reference. [e] Ref 68, oscillator strengths reported in ref 68 were converted according to eq 99 using the experimental transition wavelengths reported in Table 1 of ref 67. [f] Ref 66, relative intensities (oscillator strengths) reported in ref 66 were converted according to eq 99 using the experimental transition wavenumbers reported in Figure 1 of ref 66 for all transitions except for 7_0^1, where the transition wavenumber of ref 65 was employed; integrated cross-sections were estimated from the data reported in ref 66 assuming an amount of substance concentration of 1.47×10^{-3} mol l^{-1} of benzene at the given temperature. [g] Following ref 63, the relative intensities reported in ref 70 were converted according to eq 99 using the experimentally derived transition wavenumbers (ν_{origin}) reported in Table 6 of ref 63. [h] Ref 65, the reported relative peak heights from fluorescence excitation spectra (according to those authors, only rough estimates of the intensities) were corrected for the wavenumber dependence using the transition wavenumbers reported in Table 2 of ref 65.

Table 3. Contributions (in pm^2) of the Various e_{2g} Vibrational Normal Modes to the Total Integrated Absorption Cross-Section G_{total} (calculated according to eq 104) for the ($^1A_{1g} \rightarrow {}^1B_{2u}$) Transition of Benzene at 0 K[a]

mode	B3LYP/TZVP	camB3LYP/TZVP	HF/TZVP	CASSCF/DZP[b]	CASPT2/ANO[c]	exp.[d]	exp.[e]	exp.[f]
ν_6	2.893[2.27]	3.076[2.40]	3.988[3.18]	0.708[0.57]	[0.86]	[1.33]	[1.05]	[0.60]
ν_7	0.202	0.216	0.185	0.039				[0.04]
ν_8	0.052	0.033	0.018	0.026				
ν_9	0.014	0.008	0.000	0.016				
sum	3.160	3.334	4.191	0.789			3	

[a] Values in brackets correspond to the contribution from a limited number of members of an $a_0^1 1_0^{n'}$ progression ($a = 6, 7, 8, 9$). [b] Values obtained using the same input data set as in ref 13. [c] Ref 39, the sum of integrated absorption cross-sections as given in the present Table 2 for the $6_0^1 1_0^{n'}$ progression with $n' = 0-4$. [d] Ref 67, the sum of integrated absorption cross-sections as given in the present Table 2 for the $6_0^1 1_0^{n'}$ progression with $n' = 0-4$; if $n' = 5$ of Table 1 in ref 67 is included ($G \approx 0.1$ pm^2), one obtains a values of (1.43 pm^2). [e] Ref 68, the sum of integrated absorption cross-sections as given in the present Table 2 for the $6_0^1 1_0^{n'}$ progression with $n' = 0-4$; the value for G_{total} was obtained by converting the oscillator strength reported in ref 68 according to eq 99 by employing the transition energy for $\varepsilon_{\max}$ given in Table 2 of that work. [f] Ref 66, the sum of integrated absorption cross-sections given in the present Table 2 for the $6_0^1 1_0^{n'}$ progression with $n' = 0-4$; the partial contribution from the $7_0^1 1_0^{n'}$ progression with $n' = 0-2$ was obtained from the data of ref 66 as described in Table 2 above using the 7_0^1 transition wavenumber of ref 65 and the wavenumber increments give in Table 2 of ref 66.

CASSCF results reported in ref 13 and experimental results[65] is the 8_0^1 band, whose relative integrated band strength contribution was predicted to be too large when compared to the experimental intensity estimates obtained from peak height measurements in fluorescence excitation spectra of jet-cooled benzene.[65] The agreement seems to improve in the present work, at the price, however, of the 9_0^1 bands now being significantly less intense (on relative terms) than the experimental estimate, and even the tendency ($7_0^1 > 8_0^1 > 9_0^1$) differs from that of the experiment ($7_0^1 > 9_0^1 > 8_0^1$). When the relative integrated absorption cross-sections of 7_0^1 computed with the hybrid functionals are compared to experimental values[66] obtained from integration of the band profiles, the agreement seems almost perfect. The computed absolute values of the integrated cross-sections are, however, too large by more than a factor of 2 for the 6_0^1 transition, when judged by the experimental data of refs 67 and 68. The progression in the C−C stretching mode ν_1 built on the 6_0^1 transition appears to be too short when compared to the experiment. While the integrated band strengths of the $6_0^1 1_0^1$ are found to be the largest of the $6_0^1 1_0^{n'}$ progression at the hybrid functional level, in agreement with the experiment reported in refs 66−68, the integrated absorption cross-section ratio for $6_0^1 1_0^2/6_0$ is found to be 1/2 only, whereas experimentally the ratio is 3/4 or even larger. This too-short progression is rooted in an underestimated C−C bond length elongation upon electronic excitation.

The intensity induced by mode ν_6 via first-order Herzberg−Teller vibronic coupling appears overestimated (by about a factor of 2) according to the sum rule of eq 104. As the harmonic vibrational wavenumber of ν_6 in the electronic ground state is in reasonable agreement with experimental results (too large by about 3% on the B3LYP level), the first derivative of the electronic transition dipole moments appears not to be well-estimated or just the shape of the normal modes may not be adequately described. Interestingly, the total integrated absorption cross-section of the $\tilde{X}$ ($^1A_{1g}$) − $\tilde{A}$($^1B_{2u}$) transition is obtained at the hybrid functional level in reasonable agreement with the value deduced from the oscillator strength reported in ref 68. If one assumes this agreement to be fortuitous, it could indicate that the inducing strength of the other modes is strongly underestimated at the DFT level (which appears, however, not to be the case) or it could point to a significant higher-order Herzberg−Teller vibronic coupling contribution and possibly also a diabatic coupling contribution that gives rise to additional intensity stealing, or it could hint to some pronounced intensity redistribution due to various resonances from progressions involving ν_6 to other bands. Also, finite temperature effects, which have been neglected in the current study, and effects due to finite resolution, could play a role.

4. Conclusion

We have presented a derivation and implementation of third-order response properties that are connected to geometric derivatives of second-order response properties. The implementation is based on the exponential parametrization of the density matrix in the atomic orbital basis within time-dependent Hartree−Fock and density functional response theory. The formulation is linearly scaling for sufficiently sparse matrices.

We have demonstrated the applicability of the approach by considering the UV/vis absorption spectrum for the electronic ground state to the energetically lowest excited singlet state of benzene, a transition which is entirely dominated by vibronic coupling, here described by the first-order Herzberg−Teller corrections. The determination of the HT corrections requires the computation of the electronic excited state geometry and Hessian, as well as the geometric derivative of the electronic transition dipole moment. This is the first implementation of the analytic computation of first-order Herzberg−Teller corrections at the DFT level of theory, offering a straightforward way of overcoming the phase (and hence sign) uncertainties that can appear when determining the HT corrections by numerical derivative techniques, as well as avoiding the high computational cost, especially for systems with many degrees of freedom, of the numerical approach. Another advantage of our analytical (linear-scaling) implementation of the transition moment gradient is the possibility to combine it with a numerical derivative scheme, as already done for instance for the excited-state Hessian, to compute the second-order contributions (with respect to the nuclear coordinates) to the transition dipole. This would allow the investigation of vibronic effects beyond the linear Herzberg−Teller approximation, effects that are expected to be specifically relevant for highly symmetric systems, such as the one here investigated.

The results obtained for the Franck−Condon-forbidden electric dipole transition from the electronic ground state to the lowest excited singlet state of benzene are in qualitative agreement with experiment. Quantitatively, however, for the selected combinations of functionals (B3LYP, camB3LYP, HF) and basis set (TZVP), the total integrated absorption cross-section is found to be too large by about a factor of 2, and the predicted relative HT induction strength of the various e_{2g} modes is also not fully satisfactory. As the variability-limited accuracy of time-dependent density functional theory in the prediction of UV/vis transition wavenumbers of conjugated π systems is known, a thorough benchmark study on the performance of the various functionals in predicting quantitatively the first-order Herzberg−Teller contribution is required, for which the approaches and implementation presented in this work provide a valuable starting point.

Acknowledgment. This work has been supported by the Lundbeck Foundation and the Danish Research Council (Grant No. 9901973) and by the European Research and Training Network NANOQUANT ("Understanding Nano-Materials From the Quantum Perspective", Contract number MRTN-CT-2003-506842). S.C. acknowledges affiliation to the Instituto Nazionale Scienze dei Materiali (INSTM) and financial support from the Italian Ministero dell'Università Ricerca within the PRIN2006 (Programmi di ricerca di interesse nazionale) funding scheme. R.B. thanks the Volkswagen Foundation for financial support, acknowledges the Center for Scientific Computing (CSC) Frankfurt for computer time, and is indebted to Jürgen Stohner as well as Mark Thomson for discussions. K.R. has received support from

the Norwegian Research Council through a Centre of Excellence Grant (Grant No. 179568/V30), a YFF grant (Grant No. 162746/V00), and a VIBRON Grant (Grant No. 177558/V30). This work has also received support from NordForsk (Grant No. 070253). We also thank Jeppe Olsen and Lea S. Thøgersen for their invaluable contributions at an early stage of this project.

Appendix A. The Second-Order Renormalization Contribution

All $\boldsymbol{S}^{[3]}$ contributions to the right-hand sides in eqs 61, 62, and 63 vanish due to the fact that all of the involved vectors contain no redundant parameters, as they fulfill the projection relation 11,

$$\mathbf{a} = \mathscr{P}(\mathbf{a}) \equiv \mathbf{P}_o\mathbf{a}\mathbf{P}_v^T + \mathbf{P}_v\mathbf{a}\mathbf{P}_o^T \tag{105}$$

$$\mathbf{b}^T \equiv \mathbf{P}_v\mathbf{b}^T\mathbf{P}_o^T + \mathbf{P}_o\mathbf{b}^T\mathbf{P}_v^T \tag{106}$$

The $\boldsymbol{\eta}^{S3}$ contribution was given in eq 72

$$\boldsymbol{\eta}^{S3} = \mathbf{S}[\mathbf{D}, [\mathbf{a}, \mathbf{b}^T]_S]_S\mathbf{S} = \mathbf{S}(\mathbf{P}_o[\mathbf{a}, \mathbf{b}^T]_S - [\mathbf{a}, \mathbf{b}^T]_S\mathbf{P}_o^T)\mathbf{S} \tag{107}$$

Using the idempotency ($\mathbf{P}_o^2 = \mathbf{P}_o$ and $\mathbf{P}_v^2 = \mathbf{P}_v$) and orthogonality relations ($\mathbf{P}_o\mathbf{P}_v = \mathbf{P}_v\mathbf{P}_o = \mathbf{0}$ and $\mathbf{P}_o^T\mathbf{S}\mathbf{P}_v = \mathbf{P}_v^T\mathbf{S}\mathbf{P}_o = \mathbf{0}$), the contribution $\boldsymbol{\eta}^{S3}$ may be rewritten as

$$\boldsymbol{\eta}^{S3} = \mathbf{S}\{(\mathbf{P}_o\mathbf{a}\mathbf{P}_v^T\mathbf{S}\mathbf{P}_v\mathbf{b}^T\mathbf{P}_o^T - \mathbf{P}_o\mathbf{b}^T\mathbf{P}_v^T\mathbf{S}\mathbf{P}_v\mathbf{a}\mathbf{P}_o^T) - (\mathbf{P}_o\mathbf{a}\mathbf{P}_v^T\mathbf{S}\mathbf{P}_v\mathbf{b}^T\mathbf{P}_o^T - \mathbf{P}_o\mathbf{b}^T\mathbf{P}_v^T\mathbf{S}\mathbf{P}_v\mathbf{a}\mathbf{P}_o^T)\}\mathbf{S} = \mathbf{0} \tag{108}$$

Appendix B. The Exchange-Correlation Contributions to the Property Gradients

According to the equations given in section 2.6, the analytic computation of the geometric derivative properties here discussed requires the geometric derivative of the exchange-correlation energy functional, $\partial E_{xc}[\rho]/\partial R_\beta$, of the exchange-correlation contribution to the Kohn−Sham matrix, $\partial\mathbf{F}^{xc}/\partial R_\beta$, as well as the derivative of the exchange-correlation contribution to the (generalized) Kohn−Sham Hessian $\partial\mathbf{G}^{xc}/\partial R_\beta$. In this appendix, we derive explicit expressions for all of these exchange-correlation derivative contributions.

B.1. The Geometric Derivative of the Exchange-Correlation Energy Functional, $\partial E_{xc}[\rho]/\partial R_\beta$. The exchange-correlation energy E_{xc} is obtained from integration over space of some functional $f = f[\rho,\nabla\rho]$ of the electron density $\rho = \rho(\mathbf{r})$ and (possibly) of the gradient of the density $\nabla\rho = \nabla\rho(\mathbf{r})$:

$$E_{xc} = \int f[\rho, \nabla\rho]\, d\mathbf{r} \tag{109}$$

Differentiation with respect to a nuclear displacement R yields

$$\frac{\partial E_{xc}[\rho]}{\partial R_\beta} = \int \frac{\delta E_{xc}[\rho]}{\delta\rho(\mathbf{r})}\frac{\partial\rho(\mathbf{r})}{\partial R_\beta}\, d\mathbf{r} \tag{110}$$

The derivative of the exchange-correlation energy with respect to the density can be written:[71,72]

$$\frac{\delta E_{xc}}{\delta\rho} = \frac{\partial f[\rho,\nabla\rho]}{\partial\rho} - \nabla\frac{\partial f[\rho,\nabla\rho]}{\partial\nabla\rho} \equiv \frac{\partial f}{\partial\rho} - \nabla\frac{\partial f}{\partial\nabla\rho} \tag{111}$$

We insert eq 111 into eq 110,

$$\frac{\partial E_{xc}[\rho]}{\partial R_\beta} = \int \frac{\partial f}{\partial\rho}\frac{\partial\rho(\mathbf{r})}{\partial R_\beta}\, d\mathbf{r} - \int \frac{\partial\rho(\mathbf{r})}{\partial R_\beta}\left(\nabla\frac{\partial f}{\partial\nabla\rho}\right) d\mathbf{r} \tag{112}$$

and integrate the second term by parts according to $\int_{-\infty}^{+\infty} u\,dv = [uv]_{-\infty}^{+\infty} - \int v\,du$, with $v = \partial f/\partial\nabla\rho$, $dv = \nabla u$, and $u = \partial\rho(\mathbf{r})/\partial R_\beta$, assuming that the constant term vanishes due to the locality of f. We thus obtain

$$\frac{\partial E_{xc}[\rho]}{\partial R_\beta} = \int \frac{\partial f}{\partial\rho}\frac{\partial\rho(\mathbf{r})}{\partial R_\beta}\, d\mathbf{r} + \int \frac{\partial f}{\partial\nabla\rho}\frac{\partial\nabla\rho(\mathbf{r})}{\partial R_\beta}\, d\mathbf{r} \tag{113}$$

It is convenient to make a change of fundamental variable from $\nabla\rho$ to its norm $\xi = ||\nabla\rho||$ and consequently apply the chain rule $(\partial f(g(x)))/(\partial x) = [(\partial f)/(\partial g)][(\partial g)/(\partial x)]$ in the second term of eq 113 to obtain

$$\frac{\partial E_{xc}[\rho]}{\partial R_\beta} = \int \frac{\partial f}{\partial\rho}\frac{\partial\rho(\mathbf{r})}{\partial R_\beta}\, d\mathbf{r} + \int \frac{\partial f}{\partial\xi}\frac{\partial\xi}{\partial\nabla\rho}\frac{\partial\nabla\rho(\mathbf{r})}{\partial R_\beta}\, d\mathbf{r} \tag{114}$$

From the definition of ξ, it follows that

$$\frac{\partial\xi}{\partial\nabla\rho(\mathbf{r})} = \frac{\nabla\rho(\mathbf{r})}{\xi} \tag{115}$$

which may be inserted into eq 114, yielding the geometric derivative (i.e., the gradient) of the exchange-correlation contribution to the ground-state energy

$$\frac{\partial E_{xc}[\rho]}{\partial R_\beta} = \int \frac{\partial f}{\partial\rho}\frac{\partial\rho(\mathbf{r})}{\partial R_\beta}\, d\mathbf{r} + \int \frac{\partial f}{\partial\xi}\frac{\nabla\rho(\mathbf{r})}{\xi}\frac{\partial\nabla\rho(\mathbf{r})}{\partial R_\beta}\, d\mathbf{r} \tag{116}$$

B.2. The Exchange-Correlation Contribution to the Generalized Kohn−Sham Hessian Matrix, $\mathbf{G}^{xc}(\mathbf{M})$. Before deriving the analytic expression of the geometric derivative of the exchange-correlation contribution to the Kohn−Sham matrix, it is convenient to derive the expression of the exchange-correlation contribution to the generalized Kohn−Sham Hessian matrix:

$$G_{\mu\nu}^{xc}(\mathbf{M}) = \sum_{\rho\sigma} M_{\sigma\rho}\int \frac{\delta^2 E_{xc}}{\delta\rho(\mathbf{s})\,\delta\rho(\mathbf{r})}\,\Omega_{\mu\nu}(\mathbf{r})\,\Omega_{\rho\sigma}(\mathbf{s})\, d\mathbf{r}\, d\mathbf{s} \tag{117}$$

where $\mathbf{M}$ is a general "perturbed" density matrix, as for instance $\mathbf{D}^b$ in eq 82. Using eq 111, we obtain

$$G_{\mu\nu}^{xc}(\mathbf{M}) = \sum_{\rho\sigma} M_{\sigma\rho}\int \frac{\delta}{\delta\rho(\mathbf{s})}\frac{\partial f[\mathbf{r}]}{\partial\rho(\mathbf{r})}\Omega_{\mu\nu}(\mathbf{r})\,\Omega_{\rho\sigma}(\mathbf{s})\, d\mathbf{r}\, d\mathbf{s} - \sum_{\rho\sigma} M_{\sigma\rho}\int \frac{\delta}{\delta\rho(\mathbf{s})}\nabla_r\left(\frac{\partial f[\mathbf{r}]}{\partial\nabla\rho(\mathbf{r})}\right)\Omega_{\mu\nu}(\mathbf{r})\,\Omega_{\rho\sigma}(\mathbf{s})\, d\mathbf{r}\, d\mathbf{s} \tag{118}$$

where the subscript r in ∇_r denotes the (electronic) variable with respect to which we differentiate. Using partial integration on the second term and assuming that the constant term vanishes because f is local gives

$$G^{xc}_{\mu\nu}(\mathbf{M}) = \sum_{\rho\sigma} M_{\sigma\rho} \int \frac{\delta}{\delta\rho(\mathbf{s})} \frac{\partial f[\rho(\mathbf{r}), \nabla\rho(\mathbf{r})]}{\partial\rho(\mathbf{r})} \Omega_{\mu\nu}(\mathbf{r})\, \Omega_{\rho\sigma}(\mathbf{s})\, d\mathbf{r}\, d\mathbf{s} + \sum_{\rho\sigma} M_{\sigma\rho} \int \frac{\delta}{\delta\rho(\mathbf{s})} \frac{\partial f[\mathbf{r}]}{\partial\nabla\rho(\mathbf{r})} \nabla_r[\Omega_{\mu\nu}(\mathbf{r})] \Omega_{\rho\sigma}(\mathbf{s})\, d\mathbf{r}\, d\mathbf{s} \quad (119)$$

Using the chain rule for functional derivatives

$$\frac{\delta\mathscr{F}}{\delta g(y)} = \int \frac{\delta\mathscr{F}}{\delta f(x)} \frac{\delta f(x)}{\delta g(y)}\, dx \quad (120)$$

yields

$$G^{xc}_{\mu\nu}(\mathbf{M}) = P_1 + P_2 + P_3 + P_4 \quad (121)$$

$$P_1 = \sum_{\rho\sigma} M_{\sigma\rho} \int \frac{\delta\partial f[\mathbf{r}]}{\delta\rho(\mathbf{t})\partial\rho(\mathbf{r})} \frac{\delta\rho(\mathbf{t})}{\delta\rho(\mathbf{s})} \Omega_{\mu\nu}(\mathbf{r})\, \Omega_{\rho\sigma}(\mathbf{s})\, d\mathbf{r}\, d\mathbf{s}\, d\mathbf{t} \quad (122)$$

$$P_2 = \sum_{\rho\sigma} M_{\sigma\rho} \int \frac{\delta\partial f[\mathbf{r}]}{\delta\rho(\mathbf{t})\, \partial\nabla\rho(\mathbf{r})} \frac{\delta\rho(\mathbf{t})}{\delta\rho(\mathbf{s})} \nabla_r[\Omega_{\mu\nu}(\mathbf{r})]\, \Omega_{\rho\sigma}(\mathbf{s})\, d\mathbf{r}\, d\mathbf{s}\, d\mathbf{t} \quad (123)$$

$$P_3 = \sum_{\rho\sigma} M_{\sigma\rho} \int \frac{\delta\partial f[\mathbf{r}]}{\delta\nabla\rho(\mathbf{t})\, \partial\rho(\mathbf{r})} \frac{\delta\nabla\rho(\mathbf{t})}{\delta\rho(\mathbf{s})} \Omega_{\mu\nu}(\mathbf{r})\, \Omega_{\rho\sigma}(\mathbf{s})\, d\mathbf{r}\, d\mathbf{s}\, d\mathbf{t} \quad (124)$$

$$P_4 = \sum_{\rho\sigma} M_{\sigma\rho} \int \frac{\delta\partial f[\mathbf{r}]}{\delta\nabla\rho(\mathbf{t})\, \partial\nabla\rho(\mathbf{r})} \frac{\delta\nabla\rho(\mathbf{t})}{\delta\rho(\mathbf{s})} \nabla_r[\Omega_{\mu\nu}(\mathbf{r})]\, \Omega_{\rho\sigma}(\mathbf{s})\, d\mathbf{r}\, d\mathbf{s}\, d\mathbf{t} \quad (125)$$

Using the relation between functional and standard derivatives for composite functions

$$\frac{\delta\rho(\mathbf{t})}{\delta\rho(\mathbf{s})} = \delta(\mathbf{t} - \mathbf{s}) \quad (126)$$

$$\frac{\delta f[\rho(\mathbf{r})]}{\delta\rho(\mathbf{t})} = \frac{\partial f[\rho(\mathbf{r})]}{\partial\rho(\mathbf{r})} \delta(\mathbf{r} - \mathbf{t}) \quad (127)$$

and integrating first over $\mathbf{s}$ and then over $\mathbf{t}$, the first two terms of eq 121 become

$$P_1 + P_2 = \sum_{\rho\sigma} M_{\sigma\rho} \int \frac{\partial^2 f}{\partial\rho^2} \Omega_{\mu\nu}\Omega_{\rho\sigma}\, d\mathbf{r} + \sum_{\rho\sigma} M_{\sigma\rho} \int \frac{\partial^2 f}{\partial\rho\partial\nabla\rho} \nabla(\Omega_{\mu\nu})\, \Omega_{\rho\sigma}\, d\mathbf{r} \quad (128)$$

Using the relation

$$\frac{\delta\nabla\rho(\mathbf{t})}{\delta\rho(\mathbf{s})} = \nabla_t \frac{\delta\rho(\mathbf{t})}{\delta\rho(\mathbf{s})} = \nabla_t \delta(\mathbf{t} - \mathbf{s}) \quad (129)$$

we obtain for the last two terms

$$P_3 + P_4 = \sum_{\rho\sigma} M_{\sigma\rho} \int \frac{\delta\partial f[\mathbf{r}]}{\delta\nabla\rho(\mathbf{t})\, \partial\rho(\mathbf{r})} \times \nabla_t\delta(\mathbf{t} - \mathbf{s})\, \Omega_{\mu\nu}(\mathbf{r})\, \Omega_{\rho\sigma}(\mathbf{s})\, d\mathbf{r}\, d\mathbf{s} + \sum_{\rho\sigma} M_{\sigma\rho} \int \frac{\delta\partial f[\mathbf{r}]}{\delta\nabla\rho(\mathbf{t})\, \partial\nabla\rho(\mathbf{r})} \times \nabla_t\delta(\mathbf{t} - \mathbf{s}) \nabla_r[\Omega_{\mu\nu}(\mathbf{r})]\, \Omega_{\rho\sigma}(\mathbf{s})\, d\mathbf{r}\, d\mathbf{s} \quad (130)$$

Integrating by parts—again assuming that the constant term vanishes due to the fact that f is a local function—yields

$$P_3 + P_4 = -\sum_{\rho\sigma} M_{\sigma\rho} \int \nabla_t\left(\frac{\delta\partial f[\mathbf{r}]}{\delta\nabla\rho(\mathbf{t})\, \partial\rho(\mathbf{r})}\right) \times \delta(\mathbf{t} - \mathbf{s})\, \Omega_{\mu\nu}(\mathbf{r})\, \Omega_{\rho\sigma}(\mathbf{s})\, d\mathbf{r}\, d\mathbf{s}\, d\mathbf{t} - \sum_{\rho\sigma} M_{\sigma\rho} \times \int \nabla_t\left(\frac{\delta\partial f[\mathbf{r}]}{\delta\nabla\rho(\mathbf{t})\, \partial\nabla\rho(\mathbf{r})}\right) \times \delta(\mathbf{t} - \mathbf{s}) \nabla_r[\Omega_{\mu\nu}(\mathbf{r})]\, \Omega_{\rho\sigma}(\mathbf{s})\, d\mathbf{r}\, d\mathbf{s}\, d\mathbf{t} \quad (131)$$

Integration over $\mathbf{t}$ gives

$$P_3 + P_4 = -\sum_{\rho\sigma} M_{\sigma\rho} \int \nabla_s\left(\frac{\delta\partial f[\mathbf{r}]}{\delta\nabla\rho(\mathbf{s})\, \partial\rho(\mathbf{r})}\right) \times \Omega_{\mu\nu}(\mathbf{r})\, \Omega_{\rho\sigma}(\mathbf{s})\, d\mathbf{r}\, d\mathbf{s} - \sum_{\rho\sigma} M_{\sigma\rho} \int \nabla_s\left(\frac{\delta\partial f[\mathbf{r}]}{\delta\nabla\rho(\mathbf{s})\, \partial\nabla\rho(\mathbf{r})}\right) \times \nabla_r[\Omega_{\mu\nu}(\mathbf{r})]\, \Omega_{\rho\sigma}(\mathbf{s})\, d\mathbf{r}\, d\mathbf{s} \quad (132)$$

and yet another partial integration and an integration over $\mathbf{s}$ using eq 127 yield

$$P_3 + P_4 = \sum_{\rho\sigma} M_{\sigma\rho} \int \frac{\partial^2 f}{\partial\rho\partial\nabla\rho} \Omega_{\mu\nu} \nabla\Omega_{\rho\sigma}\, d\mathbf{r} + \sum_{\rho\sigma} M_{\sigma\rho} \int \frac{\partial^2 f}{\partial(\nabla\rho)^2} \nabla\Omega_{\mu\nu} \nabla\Omega_{\rho\sigma}\, d\mathbf{r} \quad (133)$$

The total $G^{xc}_{\mu\nu}(\mathbf{M})$ may thus be obtained from eqs 128 and 133, giving

$$G^{xc}_{\mu\nu}(\mathbf{M}) = \sum_{\rho\sigma} M_{\sigma\rho} \int \left\{ \frac{\partial^2 f}{\partial\rho^2} \Omega_{\mu\nu}\Omega_{\rho\sigma} + \frac{\partial^2 f}{\partial\rho\partial\nabla\rho} (\Omega_{\mu\nu}\nabla\Omega_{\rho\sigma} + \Omega_{\rho\sigma}\nabla\Omega_{\mu\nu}) \right\} d\mathbf{r} + \sum_{\rho\sigma} M_{\sigma\rho} \int \frac{\partial^2 f}{\partial(\nabla\rho)^2} \nabla\Omega_{\mu\nu}\, \nabla\Omega_{\rho\sigma}\, d\mathbf{r} \quad (134)$$

A transformation of variables from $\nabla\rho$ to $\xi = \|\nabla\rho\|$ yields

$$G^{xc}_{\mu\nu}(\mathbf{M}) = \sum_{\rho\sigma} M_{\sigma\rho} \int \left\{ \frac{\partial^2 f}{\partial\rho^2} \Omega_{\mu\nu}\Omega_{\rho\sigma} + \frac{\partial^2 f}{\partial\rho\partial\xi} \left(\Omega_{\mu\nu} \frac{\nabla\rho\nabla\Omega_{\rho\sigma}}{\xi} + \Omega_{\rho\sigma} \frac{\nabla\Omega_{\mu\nu}\nabla\rho}{\xi} \right) \right\} d\mathbf{r} + \sum_{\rho\sigma} M_{\sigma\rho} \int \frac{\partial^2 f}{\partial\xi^2} \frac{\nabla\Omega_{\mu\nu}\nabla_\rho}{\xi} \frac{\nabla\Omega_{\rho\sigma}\nabla\rho}{\xi}\, d\mathbf{r} \quad (135)$$

We can now use the general chain rule for second-order derivatives

$$\frac{\partial^2 f}{\partial x^2} = \frac{\partial^2 f}{\partial g^2}\left(\frac{\partial g}{\partial x}\right)^2 + \frac{\partial f}{\partial g}\frac{\partial^2 g}{\partial x^2} \tag{136}$$

to get

$$\frac{\partial^2 f}{\partial (\nabla\rho)^2} = \frac{\partial^2 f}{\partial \xi^2}\left(\frac{\partial \xi}{\partial \nabla\rho}\right)^2 + \frac{\partial f}{\partial \xi}\frac{\partial^2 \xi}{\partial (\nabla\rho)^2} = \frac{\partial^2 f}{\partial \xi^2}\left(\frac{\nabla\rho(\mathbf{r})}{\xi}\right)^2 \tag{137}$$

since

$$\frac{\partial \xi}{\partial \nabla\rho(\mathbf{r})} = \frac{\nabla\rho(\mathbf{r})}{\xi}; \qquad \frac{\partial^2 \xi}{\partial [\nabla\rho(\mathbf{r})]^2} = 0 \tag{138}$$

and do a variable transform from $\xi = \|\nabla\rho\|$ to $z = \|\nabla\rho\|^2$ and use again the general chan rule for second-order derivatives to write

$$\frac{\partial^2 f}{\partial \xi^2} = \frac{\partial^2 f}{\partial z^2}\left(\frac{\partial z}{\partial \xi}\right)^2 + \frac{\partial f}{\partial z}\frac{\partial^2 z}{\partial \xi^2} \tag{139}$$

$$\frac{\partial z}{\partial \xi} = 2\xi; \qquad \frac{\partial^2 z}{\partial \xi^2} = 2 \tag{140}$$

and thus obtain

$$G^{xc}_{\mu\nu}(\mathbf{M}) = \sum_{\rho\sigma} M_{\sigma\rho} \int \left\{ \frac{\partial^2 f}{\partial \rho^2}\Omega_{\mu\nu}\Omega_{\rho\sigma} + \frac{\partial^2 f}{\partial \rho \partial z} 2[\Omega_{\mu\nu}(\nabla\rho\nabla\Omega_{\rho\sigma}) + \Omega_{\rho\sigma}(\nabla\Omega_{\mu\nu}\nabla\rho)] \right\} d\mathbf{r} + \sum_{\rho\sigma} M_{\sigma\rho} \int \frac{\partial^2 f}{\partial z^2} 4(\nabla\Omega_{\mu\nu}\nabla\rho)\,(\nabla\Omega_{\rho\sigma}\nabla\rho)\, d\mathbf{r} + \sum_{\rho\sigma} M_{\sigma\rho} \int \frac{\partial f}{\partial z} 2\frac{\nabla\Omega_{\mu\nu}\nabla_\rho}{\xi}\frac{\nabla\Omega_{\rho\sigma}\nabla\rho}{\xi}\, d\mathbf{r} \tag{141}$$

Note the differences compared to the expression given in eq 124 of ref 28.

B.3. The Exchange-Correlation Contribution to the Differentiated Kohn−Sham Matrix, $\partial F^{xc}/\partial R_\beta$. The exchange-correlation contribution to the Kohn−Sham matrix is given by (see also eq 8)

$$F^{xc}_{\mu\nu} = \int \frac{\delta E^{xc}[\rho]}{\delta\rho(\mathbf{r})}\Omega_{\mu\nu}(\mathbf{r})\, d\mathbf{r} \tag{142}$$

The derivative of the exchange-correlation contribution to the Kohn−Sham matrix is given by

$$\frac{\partial F^{xc}_{\mu\nu}}{\partial R_\beta} = \int \frac{\delta^2 E^{xc}[\rho]}{\delta\rho(\mathbf{r})\,\delta\rho(\mathbf{s})}\frac{\partial\rho(\mathbf{s})}{\partial R_\beta}\Omega_{\mu\nu}(\mathbf{r})\, d\mathbf{r}\, d\mathbf{s} + \int \frac{\delta E^{xc}[\rho]}{\delta\rho(\mathbf{r})}\frac{\partial\Omega_{\mu\nu}(\mathbf{r})}{\partial R_\beta}\, d\mathbf{r} \tag{143}$$

which can be rewritten as

$$\frac{\partial F^{xc}_{\mu\nu}}{\partial R_\beta} = \sum_{\sigma\rho} \int D_{\sigma\rho}\frac{\delta^2 E^{xc}[\rho]}{\delta\rho(\mathbf{r})\,\delta\rho(\mathbf{s})}\frac{\partial\Omega_{\rho\sigma}(\mathbf{s})}{\partial R_\beta}\Omega_{\mu\nu}(\mathbf{r})\, d\mathbf{r}\, d\mathbf{s} + \sum_{\sigma\rho} \int \frac{\partial D_{\sigma\rho}}{\partial R_\beta}\frac{\delta^2 E^{xc}[\rho]}{\delta\rho(\mathbf{r})\delta\rho(\mathbf{s})}\Omega_{\rho\sigma}(\mathbf{s})\,\Omega_{\mu\nu}(\mathbf{r})\, d\mathbf{r}\, d\mathbf{s} + \int \frac{\delta E^{xc}[\rho]}{\delta\rho(\mathbf{r})}\frac{\partial\Omega_{\mu\nu}(\mathbf{r})}{\partial R_\beta}\, d\mathbf{r} \equiv Q_1 + Q_2 + Q_3 \tag{144}$$

Comparing the second term Q_2 with the exchange-correlation contribution to the generalized Hessian in eq 117, we can immediately write

$$Q_2 = G^{xc}_{\mu\nu}\left(\frac{\partial \mathbf{D}}{\partial R_\beta}\right) \tag{145}$$

The last term Q_3 of eq 144 is structurally similar to eq 110 and may be written as

$$Q_3 = \int \frac{\partial f}{\partial \rho}\frac{\partial\Omega_{\mu\nu}}{\partial R_\beta}\, d\mathbf{r} + \int \frac{\partial f}{\partial \xi}\frac{\nabla\rho}{\xi}\frac{\partial\nabla\Omega_{\mu\nu}}{\partial R_\beta}\, d\mathbf{r} \tag{146}$$

The first term Q_1 is similar to eq 117, except that $\Omega_{\rho\sigma}(\mathbf{s})$ should be replaced by $\partial\Omega_{\rho\sigma}(\mathbf{s})/\partial R_\beta$ and can thus be computed in analogy with terms 134 and 141:

$$Q_1 = \sum_{\rho\sigma} D_{\sigma\rho} \int \left\{ \frac{\partial^2 f}{\partial \rho^2}\Omega_{\mu\nu}\frac{\partial\Omega_{\rho\sigma}}{\partial R_\beta} + \frac{\partial^2 f}{\partial \rho \partial z} 2 \times \left[\Omega_{\mu\nu}\left(\nabla\rho\frac{\partial\nabla\Omega_{\rho\sigma}}{\partial R_\beta}\right) + \frac{\partial\Omega_{\rho\sigma}}{\partial R_\beta}(\nabla\Omega_{\mu\nu}\nabla\rho)\right] \right\} d\mathbf{r} + \sum_{\rho\sigma} D_{\sigma\rho} \int \frac{\partial^2 f}{\partial z^2} 4(\nabla\Omega_{\mu\nu}\nabla\rho)\left(\frac{\partial\Omega_{\rho\sigma}}{\partial R_\beta}\nabla\rho\right) d\mathbf{r} + \sum_{\rho\sigma} D_{\sigma\rho} \int \frac{\partial f}{\partial z^2} 2\frac{\nabla\Omega_{\mu\nu}\nabla\rho}{\xi}\frac{\nabla\dfrac{\partial\Omega_{\rho\sigma}}{\partial R_\beta}\nabla\rho}{\xi}\, d\mathbf{r} \tag{147}$$

B.4. The Additional Exchange-Correlation Contribution to the Quadratic Response $T^{xc}_{\mu\nu}(\mathbf{N},\mathbf{M})$. As a last preliminary step to be able to compute the derivative of the exchange-correlation contribution to the generalized Kohn−Sham matrix Hessian, we derive here the explicit expression for the additional exchange-correlation contribution required in computing quadratic response properties:[41]

$$T^{xc}_{\mu\nu}(\mathbf{N},\mathbf{M}) = \sum_{\rho\sigma\eta\varepsilon} M_{\sigma\rho}N_{\varepsilon\eta} \int \Omega_{\eta\varepsilon}(\mathbf{t})\,\Omega_{\rho\sigma}(\mathbf{s})\,\Omega_{\mu\nu}(\mathbf{r}) \times \frac{\delta^2 v_{xc}(\mathbf{r})}{\delta\rho(\mathbf{s})\,\delta\rho(\mathbf{t})}\, d\mathbf{r}\, d\mathbf{s}\, d\mathbf{t} \tag{148}$$

where $\mathbf{M}$ and $\mathbf{N}$ are general "perturbed" density matrices, like $\mathbf{D}^b$ in eq 82. Defining

$$\kappa(\mathbf{r}) = \sum_{\sigma\rho} M_{\sigma\rho}\,\Omega_{\rho\sigma}(\mathbf{r}) \tag{149}$$

$$\nabla\kappa(\mathbf{r}) = \sum_{\sigma\rho} M_{\sigma\rho}\nabla\Omega_{\rho\sigma}(\mathbf{r}) \tag{150}$$

$$\tau(\mathbf{r}) = \sum_{\sigma\rho} N_{\sigma\rho}\,\Omega_{\rho\sigma}(\mathbf{r}) \tag{151}$$

$$\nabla\tau(\mathbf{r}) = \sum_{\sigma\rho} N_{\sigma\rho}\nabla\Omega_{\rho\sigma}(\mathbf{r}) \tag{152}$$

we can write, in a shorthand notation,

$$T^{\mathrm{xc}}_{\mu\nu} = \int \tau(\mathbf{t})\,\kappa(\mathbf{s})\,\Omega_{\mu\nu}(\mathbf{r})\,\frac{\delta^2 v_{\mathrm{xc}}(\mathbf{r})}{\delta\rho(\mathbf{s})\,\delta\rho(\mathbf{t})}\,\mathrm{d}\mathbf{r}\,\mathrm{d}\mathbf{s}\,\mathrm{d}\mathbf{t} \tag{153}$$

The first functional derivative yields

$$T^{\mathrm{xc}}_{\mu\nu} = \int \left[\tau(\mathbf{t})\frac{\delta}{\delta\rho(\mathbf{t})}\frac{\partial^2 f}{\partial\rho^2}\Omega_{\mu\nu}\kappa + \tau(\mathbf{t})\frac{\delta}{\delta\rho(\mathbf{t})}\frac{\partial^2 f}{\partial\rho\partial\nabla\rho}(\Omega_{\mu\nu}\nabla\kappa + \kappa\nabla\Omega_{\mu\nu})\right]\mathrm{d}\mathbf{r}\,\mathrm{d}\mathbf{t} + \int \tau(\mathbf{t})\frac{\delta}{\delta\rho(\mathbf{t})}\frac{\partial^2 f}{\partial(\nabla\rho)^2}\nabla\Omega_{\mu\nu}\nabla\kappa\,\mathrm{d}\mathbf{r}\,\mathrm{d}\mathbf{t} \tag{154}$$

Doing the same for the second functional derivative, we obtain

$$T^{\mathrm{xc}}_{\mu\nu} = \int \left(\frac{\partial^3 f}{\partial\rho^3}\kappa\tau + \frac{\partial^3 f}{\partial\rho^2\partial\nabla\rho}\kappa\nabla\tau + \frac{\partial^3 f}{\partial\rho^2\partial\nabla\rho}\tau\nabla\kappa + \frac{\partial^3 f}{\partial\rho\partial(\nabla\rho)^2}\nabla\kappa\nabla\tau\right)\Omega_{\mu\nu}\,\mathrm{d}\mathbf{r} + \int \frac{\partial^3 f}{\partial\rho^2\partial\nabla\rho}\tau\kappa\nabla\Omega_{\mu\nu}\,\mathrm{d}\mathbf{r} + \int \frac{\partial^3 f}{\partial\rho\partial(\nabla\rho)^2}\nabla\tau\kappa\nabla\Omega_{\mu\nu}\,\mathrm{d}\mathbf{r} + \int \frac{\partial^3 f}{\partial\rho\partial(\nabla\rho)^2}\nabla\Omega_{\mu\nu}\nabla\kappa\tau\,\mathrm{d}\mathbf{r} + \int \frac{\partial^3 f}{\partial(\nabla\rho)^3}\nabla\Omega_{\mu\nu}\nabla\kappa\nabla\tau\,\mathrm{d}\mathbf{r} \tag{155}$$

A variable transformation from $\nabla\rho$ to $\xi = \|\nabla\rho\|$ gives

$$T^{\mathrm{xc}}_{\mu\nu} = \int \left(\frac{\partial^3 f}{\partial\rho^3}\kappa\tau + \frac{\partial^3 f}{\partial\rho^2\partial\xi}\frac{\nabla\rho}{\xi}\kappa\nabla\tau + \frac{\partial^3 f}{\partial\rho^2\partial\xi}\tau\nabla\kappa\frac{\nabla\rho}{\xi} + \frac{\partial^3 f}{\partial\rho\partial\xi^2}\left(\frac{\nabla\rho}{\xi}\right)^2\nabla\kappa\nabla\tau\right)\Omega_{\mu\nu}\,\mathrm{d}\mathbf{r} + \int \frac{\partial^3 f}{\partial\rho^2\partial\xi}\frac{\nabla\rho}{\xi}\tau\kappa\nabla\Omega_{\mu\nu}\,\mathrm{d}\mathbf{r} + \int \frac{\partial^3 f}{\partial\rho\partial\xi^2}\left(\frac{\nabla\rho}{\xi}\right)^2\nabla\tau\kappa\nabla\Omega_{\mu\nu}\,\mathrm{d}\mathbf{r} + \int \frac{\partial^3 f}{\partial\rho^2\partial\xi}\left(\frac{\nabla\rho}{\xi}\right)^2\nabla\Omega_{\mu\nu}\nabla\kappa\tau\,\mathrm{d}\mathbf{r} + \int \frac{\partial^3 f}{\partial\xi^3}\left(\frac{\nabla\rho}{\xi}\right)^3\nabla\Omega_{\mu\nu}\nabla\kappa\nabla\tau\,\mathrm{d}\mathbf{r} \tag{156}$$

From $(\partial f)/(\partial\nabla\rho) = [(\partial f)/(\partial\xi)][(\partial\xi)/(\partial\nabla\rho)] = (\nabla\rho)/(\xi)$ and the general chain rule for second-order derivatives in eq 136, we can write

$$\frac{\partial^3 f}{\partial(\nabla\rho)^3} = \frac{\partial^3 f}{\partial\xi^3}\left(\frac{\partial\xi}{\partial\nabla\rho}\right)^3 + 3\frac{\partial^2 f}{\partial\xi^2}\frac{\partial^2\xi}{\partial(\nabla\rho)^2}\frac{\partial\xi}{\partial\nabla\rho} + \frac{\partial f}{\partial\xi}\frac{\partial^3\xi}{\partial(\nabla\rho)^3} = \frac{\partial^3 f}{\partial\xi^3}\left(\frac{\nabla\rho}{\xi}\right)^3 \tag{157}$$

since

$$\frac{\partial\xi}{\partial\nabla\rho} = \frac{\nabla\rho(\mathbf{r})}{\xi} \tag{158}$$

$$\frac{\partial^2\xi}{\partial(\nabla\rho)^2} = 0 \tag{159}$$

$$\frac{\partial^3\xi}{\partial(\nabla\rho)^3} = 0 \tag{160}$$

Another variable transformation from $\xi = \|\nabla\rho\|$ to $z = \|\nabla\rho\|^2$ and application of the chain rule for higher-order derivatives gives

$$\frac{\partial f}{\partial\xi} = \frac{\partial f}{\partial z}\frac{\partial z}{\partial\xi} = \frac{\partial f}{\partial z}2\xi \tag{161}$$

$$\frac{\partial^2 f}{\partial\xi^2} = \frac{\partial^2 f}{\partial z^2}\left(\frac{\partial z}{\partial\xi}\right)^2 + \frac{\partial f}{\partial z}\frac{\partial^2 z}{\partial\xi^2} = \frac{\partial^2 f}{\partial z^2}4\xi^2 + \frac{\partial f}{\partial z}2 \tag{162}$$

$$\frac{\partial^3 f}{\partial\xi^3} = \frac{\partial^3 f}{\partial z^3}\left(\frac{\partial z}{\partial\xi}\right)^3 + 3\frac{\partial^2 f}{\partial z^2}\frac{\partial^2 z}{\partial\xi^2}\frac{\partial z}{\partial x} + \frac{\partial f}{\partial z}\frac{\partial^3 z}{\partial\xi^3} = \frac{\partial^3 f}{\partial z^3}8\xi^3 + 3\frac{\partial^2 f}{\partial z^2}4\xi \tag{163}$$

$$\frac{\partial z}{\partial\xi} = 2\xi \tag{164}$$

$$\frac{\partial^2 z}{\partial\xi^2} = 2 \tag{165}$$

and we obtain

$$T^{\mathrm{xc}}_{\mu\nu} = \int \left(\frac{\partial^3 f}{\partial\rho^3}\kappa\tau + \frac{\partial^3 f}{\partial\rho^2\partial z}2\nabla\rho\kappa\nabla\tau + \frac{\partial^3 f}{\partial\rho^2\partial z}\tau\nabla\kappa 2\nabla\rho + \frac{\partial^3 f}{\partial\rho\partial z^2}4(\nabla\rho)^2\nabla\kappa\nabla\tau + \frac{\partial^2 f}{\partial\rho\partial z}2\left(\frac{\nabla\rho}{\xi}\right)^2\nabla\kappa\nabla\tau\right)\Omega_{\mu\nu}\,\mathrm{d}\mathbf{r} + \int \frac{\partial^3 f}{\partial\rho^2\partial z}2\nabla\rho\tau\kappa\nabla\Omega_{\mu\nu}\,\mathrm{d}\mathbf{r} + \int \frac{\partial^3 f}{\partial\rho\partial z^2}4(\nabla\rho)^2\nabla\tau\kappa\nabla\Omega_{\mu\nu}\,\mathrm{d}\mathbf{r} + \int \frac{\partial^2 f}{\partial\rho\partial z}2\left(\frac{\nabla\rho}{\xi}\right)^2\nabla\tau\kappa\nabla\Omega_{\mu\nu}\,\mathrm{d}\mathbf{r} + \int \frac{\partial^3 f}{\partial\rho\partial z^2}4(\nabla\rho)^2\nabla\Omega_{\mu\nu}\nabla\kappa\tau\,\mathrm{d}\mathbf{r} + \int \frac{\partial^2 f}{\partial\rho\partial z}2\left(\frac{\nabla\rho}{\xi}\right)^2\nabla\Omega_{\mu\nu}\nabla\kappa\tau\,\mathrm{d}\mathbf{r} + \int \frac{\partial^3 f}{\partial z^3}8(\nabla\rho)^3\nabla\Omega_{\mu\nu}\nabla\kappa\nabla\tau\,\mathrm{d}\mathbf{r} + \int \frac{\partial^2 f}{\partial z^2}3\cdot 4\xi\left(\frac{\nabla\rho}{\xi}\right)^3\nabla\Omega_{\mu\nu}\nabla\kappa\nabla\tau\,\mathrm{d}\mathbf{r} \tag{166}$$

B.5. The Derivative of the Kohn−Sham Contribution to the Generalized Hessian $\partial G^{xc}_{\mu\nu}(\mathbf{M})/\partial R_\beta$.

$$\begin{aligned}\frac{\partial G^{xc}_{\mu\nu}(\mathbf{M})}{\partial R_\beta} = & \sum_{\rho\sigma}\frac{\partial M_{\sigma\rho}}{\partial R_\beta}\int\frac{\delta^2 E^{xc}}{\delta\rho(\mathbf{s})\,\delta\rho(\mathbf{r})}\times \\ & \Omega_{\mu\nu}(\mathbf{r})\,\Omega_{\rho\sigma}(\mathbf{s})\,d\mathbf{r}\,d\mathbf{s} \\ & + \sum_{\rho\sigma\eta\varepsilon} M_{\sigma\rho}\int\frac{\delta^3 E^{xc}}{\delta\rho(\mathbf{t})\,\delta\rho(\mathbf{s})\,\delta\rho(\mathbf{r})}\frac{\partial D_{\varepsilon\eta}}{\partial R_\beta}\times \\ & \Omega_{\eta\varepsilon}(\mathbf{t})\,\Omega_{\mu\nu}(\mathbf{r})\,\Omega_{\rho\sigma}(\mathbf{s})\,d\mathbf{r}\,d\mathbf{s}\,d\mathbf{t} \\ & + \sum_{\rho\sigma\varepsilon\eta} D_{\varepsilon\eta}M_{\sigma\rho}\int\frac{\delta^3 E^{xc}}{\delta\rho(\mathbf{t})\,\delta\rho(\mathbf{s})\,\delta\rho(\mathbf{r})}\frac{\partial\Omega_{\eta\varepsilon}(\mathbf{t})}{\partial R_\beta}\times \\ & \Omega_{\mu\nu}(\mathbf{r})\,\Omega_{\rho\sigma}(\mathbf{s})\,d\mathbf{r}\,d\mathbf{s}\,d\mathbf{t} \\ & + \sum_{\rho\sigma} M_{\sigma\rho}\int\frac{\delta^2 E^{xc}}{\delta\rho(\mathbf{s})\,\delta\rho(\mathbf{r})}\frac{\partial\Omega_{\mu\nu}(\mathbf{r})}{\partial R_\beta}\times \\ & \Omega_{\rho\sigma}(\mathbf{s})\,d\mathbf{r}\,d\mathbf{s} \\ & + \sum_{\rho\sigma} M_{\sigma\rho}\int\frac{\delta^2 E^{xc}}{\delta\rho(\mathbf{s})\,\delta\rho(\mathbf{r})}\Omega_{\mu\nu}(\mathbf{r})\frac{\partial\Omega_{\rho\sigma}(\mathbf{s})}{\partial R_\beta}\,d\mathbf{r}\,d\mathbf{s} \\ = & \; Z_1 + Z_2 + Z_3 + Z_4 + Z_5 \end{aligned} \tag{167}$$

From consideration of the structure of the five terms above, it may be seen that

$$Z_1 = G^{xc}_{\mu\nu}\left(\frac{\partial\mathbf{M}}{\partial R_\beta}\right) \tag{168}$$

$$Z_2 = T^{xc}_{\mu\nu}\left(\frac{\partial\mathbf{D}}{\partial R_\beta},\mathbf{M}\right) \tag{169}$$

The term Z_3 is similar to eq 59 (i.e., eq 148) except that $\Omega_{\eta\epsilon}(\mathbf{t})$ should be replaced with $[\partial\Omega_{\eta\epsilon}(\mathbf{t})]/(\partial R_\beta)$. The terms Z_4 and Z_5 are similar to eq 117 except that $\Omega_{\mu\nu}(\mathbf{r})$ and $\Omega_{\rho\sigma}(\mathbf{s})$ should be replaced with $[\partial\Omega_{\mu\nu}(\mathbf{r})]/(\partial R_\beta)$ and $[\partial\Omega_{\rho\sigma}(\mathbf{s})]/(\partial R_\beta)$, respectively.

References

(1) Helgaker, T. *Int. J. Quantum Chem.* **1982**, *21*, 939–940.

(2) Bartlett, R. J. In *Geometrical Derivatives of Energy Surfaces and Molecular Properties*; Jørgensen, P., Simons, J., Eds.; Reidel: Dordrecht, The Netherlands, 1986.

(3) Helgaker, T.; Ruud, K.; Bak, K. L.; Jørgensen, P.; Olsen, J. *Faraday Discuss.* **1994**, *99*, 165.

(4) Pulay, P. In *Modern Electronic Structure Theory, Part II*; Yarkony, D. R., Ed.; World Scientific: Singapore, 1995.

(5) Quinet, O.; Champagne, B. *J. Chem. Phys.* **2001**, *115* (14), 6293–6299.

(6) Quinet, O.; Champagne, B.; Kirtman, B. *J. Comput. Chem.* **2001**, *22*, 1920–1932.

(7) Quinet, O.; Champagne, B.; Kirtman, B. *J. Chem. Phys.* **2003**, *117* (6), 2481–2488.

(8) Liégeois, V.; Ruud, K.; Champagne, B. *J. Chem. Phys.* **2007**, *127* (1−6), 204105.

(9) Rappoport, D.; Furche, F. *J. Chem. Phys.* **2007**, *126*, 201104.

(10) Barron, L. D. *Molecular Light Scattering and Optical Activity*, 2nd ed. revised and enlarged; Cambridge University Press: Cambridge, U. K., 2004.

(11) Thorvaldsen, A. J.; Ferrighi, L.; Ruud, K.; Ågren, H.; Coriani, S.; Jørgensen, P. *Phys. Chem. Chem. Phys.* **2009**, *11*, 2293–2304.

(12) Ruud, K.; Thorvaldsen, A. *Chirality* **2009**, *21*, S54–S67.

(13) Berger, R.; Fisher, C.; Klessinger, M. *J. Phys. Chem. A* **1998**, *112*, 7157–7167.

(14) Lin, N.; Zhao, X.; Rizzo, A.; Luo, Y. *J. Chem. Phys.* **2007**, *127*, 244509.

(15) Santoro, F.; Lami, A.; Improta, R.; Bloino, J.; Barone, V. *J. Chem. Phys.* **2008**, *128*, 224311.

(16) Helgaker, T.; Jørgensen, P. Calculation of Geometrical Derivatives in Molecular Electronic Structure Theory. In *Methods in Computational Molecular Physics*; Wilson, S., Diercksen, G. H. F., Eds.; Plenum Press: New York, 1992.

(17) Helgaker, T.; Jørgensen, P. Analytical Calculation of Geometrical Derivatives in Molecular Electronic Structure Theory. In *Adv. Quantum Chem.*; Academic Press: New York, 1988; Vol 19.

(18) Jørgensen, P.; Helgaker, T. *J. Chem. Phys.* **1988**, *89*, 1560–1570.

(19) Helgaker, T.; Jørgensen, P. *Theor. Chim. Acta* **1989**, *75*, 111–127.

(20) Helgaker, T.; Jørgensen, P.; Handy, N. *Theor. Chim. Acta* **1989**, *76*, 227–245.

(21) Sasagane, K.; Aiga, F.; Itoh, R. *J. Chem. Phys.* **1993**, *99*, 3738.

(22) Christiansen, O.; Hättig, C.; Jørgensen, P. *Int. J. Quantum Chem.* **1998**, *68*, 1.

(23) Furche, F.; Ahlrichs, R. *J. Chem. Phys.* **2002**, *117*, 7433.

(24) Szabo, A.; Ostlund, N. S. *Modern Quantum Chemistry. Introduction to Advanced Electronic Structure Theory*; Dover Publications: Mineola, NY, 1996.

(25) Helgaker, T.; Jørgensen, P.; Olsen, J. *Molecular Electronic-Structure Theory*; Wiley: Chichester, U. K., 2000.

(26) Koch, H.; Jensen, H. J. A.; Jørgensen, P.; Helgaker, T.; Scuseria, G. E.; Schaefer, H. F., III. *Phys. Chem. Chem. Phys.* **2009**, *11*, 2293–2304.

(27) Hald, K.; Halkier, A.; Jørgensen, P.; Coriani, S.; Hättig, C.; Helgaker, T. *J. Chem. Phys.* **2003**, *118*, 2985.

(28) Kjærgaard, T.; Jørgensen, P.; Thorvaldsen, A. J.; Salek, P.; Coriani, S. *J. Chem. Theory Comput.* **2009**, *5*, 1997–2020.

(29) Hättig, C.; Christiansen, O.; Jørgensen, P. *J. Chem. Phys.* **1998**, *108*, 8331–8354.

(30) Hättig, C.; Jørgensen, P. *J. Chem. Phys.* **1998**, *109*, 9219.

(31) Sałek, P.; Vahtras, O.; Helgaker, T.; Ågren, H. *J. Chem. Phys.* **2002**, *117*, 9630.

(32) Thorvaldsen, A.; Ruud, K.; Kristensen, K.; Jørgensen, P.; Coriani, S. *J. Chem. Phys.* **2008**, *129*, 214108.

(33) Larsen, H.; Jørgensen, P.; Olsen, J.; Helgaker, T. *J. Chem. Phys.* **2000**, *113*, 8908.

(34) Coriani, S.; Høst, S.; Jansík, B.; Thøgersen, L.; Olsen, J.; Jørgensen, P.; Reine, S.; Pawlowski, F.; Helgaker, T.; Sałek, P. *J. Chem. Phys.* **2007**, *126*, 154108.

(35) Helgaker, T.; Larsen, H.; Olsen, J.; Jørgensen, P. *Chem. Phys. Lett.* **2000**, *327*, 397.

(36) Coriani, S.; Hättig, C.; Jørgensen, P.; Helgaker, T. *J. Chem. Phys.* **2000**, *113*, 3561.

(37) Kjærgaard, T.; Jansík, B.; Jørgensen, P.; Coriani, S.; Michl, J. *J. Phys. Chem. A* **2007**, *111*, 11278–11286.

(38) Thorvaldsen, A.; Ruud, K.; Jaszunski, M. *J. Phys. Chem. A* **2008**, *112*, 11942.

(39) Bernhardsson, A.; Forsberg, N.; Malmqvist, P.-Å.; Roos, B. *J. Chem. Phys.* **2000**, *112*, 2798–2809.

(40) Larsen, H.; Helgaker, T.; Jørgensen, P.; Olsen, J. *J. Chem. Phys.* **2001**, *115*, 10344.

(41) Kjærgaard, T.; Jørgensen, P.; Olsen, J.; Coriani, S.; Helgaker, T. *J. Chem. Phys.* **2008**, *129*, 054106.

(42) Olsen, J.; Jørgensen, P. Time-Dependent Response Theory with Applications to Self-Consistent Field and Multiconfigurational Self-Consistent Field Wave Functions. In *Modern Electronic Structure Theory, Part II*; Yarkony, D. R., Ed.; World Scientific: Singapore, 1995.

(43) Hettema, H.; Jensen, H. J. A.; Jørgensen, P.; Olsen, J. *J. Chem. Phys.* **1992**, *97*, 1174.

(44) Helgaker, T. U.; Jensen, H.; Jørgensen, P. *J. Chem. Phys.* **1986**, *182*, 6280.

(45) DALTON, an ab initio electronic structure program, Release 2.0, 2005. See http://www.kjemi.uio.no/software/dalton/dalton.html.

(46) Sałek, P.; Høst, S.; Thøgersen, L.; Jørgensen, P.; Manninen, P.; Olsen, J.; Jansík, B.; Reine, S.; Pawlowski, F.; Tellgren, E.; Helgaker, T.; Coriani, S. *J. Chem. Phys.* **2007**, *126*, 114110.

(47) Cohen, E.; Cvitas, T.; Frey, J.; Holmstrom, B.; Kuchitsu, K.; Marquardt, R.; Mills, I.; Pavese, F.; Quack, M.; Stohner, J.; Strauss, H.; Takami, M.; Thor, A. *Quantities, Units, and Symbols in Physical Chemistry*, 3rd ed., also known as the IUPAC Green Book; RSC Publishing: London, U. K., 2007.

(48) Crawford, B., Jr. *J. Chem. Phys.* **1958**, *29*, 1042–1045.

(49) Orlandi, G.; Siebrand, W. *Chem. Phys. Lett.* **1972**, *15*, 465–468.

(50) Huh, J. S.; Stuber, J. L.; Berger, R. Vibronic Transitions in Large Molecular Systems: The Thermal Time-Correlation Function and Rigorous Prescreening of Herzberg-Teller Terms. To be published.

(51) Jankowiak, H.-C.; Stuber, J. L.; Berger, R. *J. Chem. Phys.* **2007**, *127*, 234101.

(52) Huh, J. S.; Stuber, J. L.; Berger, R. Vibronic Transitions in Large Molecular Systems: Prescreening Conditions for Franck−Condon Factors at Finite Temperature and the Thermal Time-Correlation Function. To be published.

(53) Becke, A. D. *J. Chem. Phys.* **1993**, *98*, 5648–5652.

(54) Stephens, P. J.; Devlin, F. J.; Chabalowski, C. F.; Frisch, M. J. *J. Phys. Chem.* **1994**, *98*, 11623–11627.

(55) Yanai, T.; Tew, D. P.; Handy, N. C. *Chem. Phys. Lett.* **2004**, *393*, 51.

(56) Schäfer, A.; Huber, C.; Ahlrichs, R. *J. Chem. Phys.* **1994**, *100*, 5829–5835.

(57) Lindh, R.; Malmqvist, P.-Å.; Gagliardi, L. *Theor. Chem. Acc.* **2001**, *106*, 178–187.

(58) Lebedev, V. I. *Zh. Vychisl. Mat. Mat. Fiz.* **1975**, *15*, 48.

(59) Lebedev, V. I. *Zh. Vychisl. Mat. Mat. Fiz.* **1976**, *16*, 293.

(60) Lebedev, V. I. *Sibirsk. Mat. Zh.* **1977**, *18*, 132.

(61) Frigo, M.; Johnson, S. G. *Proc. IEEE* **2005**, *93* (2), 216–231, Special issue on "Program Generation, Optimization, and Platform Adaptation." .

(62) Wilson, E. B. *Phys. Rev.* **1934**, *45*, 707–711.

(63) Callomon, J.; Dunn, T.; Mills, I. *Trans. R. Soc., London* **1966**, *259*, 499–532.

(64) Christiansen, O.; Stanton, J.; Gauss, J. *J. Chem. Phys.* **1998**, *108*, 3987.

(65) Stephenson, T.; Radloff, P.; Rice, S. *J. Chem. Phys.* **1984**, *81*, 1060–1072.

(66) Fischer, G.; Jakobson, S. *Mol. Phys.* **1979**, *38*, 299–308.

(67) Hiraya, A.; Shobatake, K. *J. Chem. Phys.* **1991**, *94*, 7700.

(68) Pantos, E.; Philis, J.; Bolovinos, A. *J. Mol. Spectrosc.* **1978**, *72*, 36.

(69) Page, R.; Shen, Y.; Lee, Y. *J. Chem. Phys.* **1988**, *88*, 5362–5376.

(70) Radle, W.; Beck, C. *J. Chem. Phys.* **1940**, *7*, 507–513.

(71) Parr, R. G.; Yang, W. *Density-Functional Theory of Atoms and Molecules*; Oxford Science Publications: Oxford, U. K., 1989.

(72) Sałek, P.; Hesselmann, A. *J. Comput. Chem.* **2007**, *28*, 2569–2575.

CT900506C